Biodegradable glutaraldehyde-cross-linked casein conduit promotes regeneration after peripheral nerve injury in adult rats

Walter Wang[a], Jia-Horng Lin[b], Chin-Chuan Tsai[c,d], Hao-Che Chuang[e], Chien-Yi Ho[f,#], Chun-Hsu Yao[a,g,#], Yueh-Sheng Chen[a,*,#]

[a]*Laboratory of Biomaterials, School of Chinese Medicine, China Medical University, Taichung, Taiwan*
[b]*Laboratory of Fiber Application and Manufacturing, Graduated Institute of Textile Engineering, Feng Chia University, Taichung Taiwan*
[c]*School of Chinese Medicine for Post-Baccalaureate, I-Shou University, Kaohsiung, Taiwan*
[d]*Chinese Medicine Department, E-DA Hospital, Kaohsiung, Taiwan*
[e]*Department of Neurosurgery, China Medical University Hospital, China Medical University, Taichung, Taiwan*
[f]*Department of Family Medicine, China Medical University Hospital, China Medical University, Taichung, Taiwan*
[g]*Department of Biomedical Imaging and Radiological Science, China Medical University, Taichung, Taiwan*

#Those authors contributed equally to this work.

*Corresponding author: Yueh-Sheng Chen, Ph.D.
Laboratory of Biomaterials, School of Chinese Medicine,
China Medical University, Taichung, Taiwan
Tel.: 886-4-22053366 ext. 3308; Fax: 886-4-22032295
E-mail: yuehsc@mail.cmu.edu.tw

Abstract

In this study, glutaraldehyde-cross-linked casein protein (GCC) was used for the first time to make a biodegradable conduit for peripheral nerve repair. The GCC was highly stable with a sufficiently high level of mechanical properties and it was non-toxic and non-apoptotic which could maintain the survival and outgrowth of Schwann cells. Noninvasive bioluminescence imaging accompanied with histochemical assessment showed the GCC was highly biocompatible after subcutaneous implantation in transgenic mice. Electrophysiology, labeling of calcitonin gene-related peptide in the lumbar spinal cord and histology analysis also showed a rapid morphological and functional recovery for disrupted rat sciatic nerves repaired with the GCC conduits. Therefore, we conclude that the GCC can offer great nerve regeneration characteristics and can be a promising material for the successful repair of peripheral nerve defects.

Keywords: Casein; Glutaraldehyde; Nerve conduit; Nerve regeneration; Nerve injury

Introduction

For improving peripheral nerve regeneration, the development of biomaterials to make nerve bridge conduits has attracted considerable attention in recent years. A

nerve bridge technique is the introduction of both ends of the injured nerve stumps into a tubular chamber, which can offer the advantages of aiding guidance of growing fibers along appropriate paths by mechanical orientation and confinement, and enhancing the precision of stump approximation. Several synthetic materials, either nondegradable[1-3] or biodegradable,[4-6] have been used as a nerve conduit. The main objection for using nondegradable conduits is that they remain *in situ* as foreign bodies after the nerve has regenerated and may require a second surgery to remove the conduits, causing possible damage to the nerve.[7,8] Therefore, biodegradable conduits seem a more promising alternative to reconstruct nerve gaps. An ideal biodegradable conduit should maintain its structural integrity, permitting cell infiltration and subsequent tissue growth during the regenerative processes.[9] Nowadays, several biodegradable nerve conduits have been approved by the Food and Drug Administration (FDA) for nerve repair in clinics, such as SaluBridge® (polyvinyl alcohol), Neurotube® (polyglycolic acid), and NeuraGen® (collagen). In the present study, we developed a novel protein-based biodegradable conduit for nerve repair. For this purpose, casein, a predominant phosphoprotein accounting for nearly 80% of proteins in cow milk was crosslinked by glutaraldehyde.[10,11] To understand physical characteristics of the glutaraldehyde-crosslinked casein (GCC) conduits, we evaluated their mechanical function, water uptake ratio, and hydrophilicity. Cytotoxic testing

and terminal deoxynucleotidyl transferase dUTP nick end labeling (TUNEL) of the conduits were determined by using the Schwann cell line, which has been extensively adopted to study neural cell differentiation,[12-14] to study cell viability upon exposure to the substances released from soaked GCC conduits. The inflammatory response is a key component in the biocompatibility of biomaterials. Among the factors that control the development of inflammation is a critical molecule nuclear factor-κB (NF-κB).[15,16] Therefore, NF-κB-dependent luminescent signal in transgenic mice carrying the luciferase genes was used as the guide to assess the host-GCC interaction. In addition, it has been reported that regeneration process may be directly impaired in regenerative microenvironment caused by deficits in action of vasoactive neuropeptides such as calcitonin gene-related peptide (CGRP).[17,18] Since the CGRP expression has an impact on nature of peripheral nerve regeneration[19] that we tested the possibility that constructed GCC conduits promote axonal regeneration and functional restoration by examining the CGRP in the lumbar spinal cord by immunohistochemistry, and correlating morphometric and electrophysiological data in 1 cm Sprague-Dawley (SD) rat sciatic nerve defect.

Experimental Part

Fabrication of GCC Conduits

A 20% (w/w) solution of casein (Sigma #C5890, Saint Louis, MO) in 0.2 M Na_2HPO_4 buffer was prepared by magnetic stirring. A silicone rubber tube (1.96 mm OD; Helix Medical, Inc., Carpinteria, CA) was used as a mandrel vertically dipped into the casein solution at a constant speed where it remained for 2 min. The mandrel was then withdrawn slowly and allowed to stand for 25 min for air-drying. The mandrel was rotated horizontally consistently to reduce variations in the wall thickness along the axis of the tube. Four coating steps were used and the casein-coated mandrel was then immersed in 0.1% (w/w) solution of glutaraldehyde (Sigma #G5882, Saint Louis, MO) for 30 min for cross-linking. The coated mandrel was rinsed twice with distilled water, dehydrated for 10 min with 95% of ethanol, and air-drying for 1 week. The GCCs were slipped off the silicone rubber mandrel and cut to 12 mm length. To allow fixation of the nerve tissue to the conduit, two small holes were drilled at both ends of the GCCs. Finally, the GCCs were sterilized with 25 kGy of γ-ray for subsequent implantation.

Cross-linking Degree of GCC Conduits

Ninhydrin assay was used to evaluate the cross-linking degree of GCC conduits. Ninhydrin (2,2-dihydroxy-1,3-indanedione) was used to determine the amount of amino groups of each test sample. The test GCC conduits were heated with a

ninhydrin solution for 20 min. After heating with ninhydrin, the optical absorbance of the solution was recorded using a spectrophotometer (Model Genesys™ 10, Spectronic Unicam, New York, NY) at 570 nm (wavelength of the blue-purple color) using casein at various known concentrations as standard. The amount of free amino groups in the residual casein, after heating with ninhydrin, is proportional to the optical absorbance of the solution. The cross-linking degree of GCC conduits was then determined.

Macroscopic Observation of GCC Conduits

To examine the morphology of the GCC explants with scanning electron microscopy (SEM), the samples were gold-coated using a Hitachi E-1010 Ion Sputter and micrographs were obtained using a Hitachi S3000N scanning electron microscope at an accelerating voltage of 5 kV.

Mechanical Function of GCC Samples

The mechanical properties of GCC were determined in a dry condition. All test samples were preconditioned at 50% humidity and 23°C for 48 h. The maximum tensile strength was determined by the universal testing machines (AG-IS, Shimadzu Co., Japan). All test samples, cut into dumbbell shape (Fig. 1), were pulled at an

extension rate of 0.6 mm/min. Measurements were made five times for each sample and averages were reported.

Water Contact Angle Analysis of GCC Samples

Drops of distilled water were placed on the GCC films and contact angles were measured using a static contact angle meter (CA-D, Kyowa, Japan). An auto pipette was employed with the meter to ensure that the volume of the distilled water droplet was the same (20 μL) for each specimen.

Water Uptake Ratio of GCC Conduits

The weight equilibrium water uptake ratio was experimentally determined using the following equation:

water uptake ratio = $(Wt-W_0)/W_0$

where Wt is the weight of the swollen test sample and W_0 is the weight of the dried test sample. The measuring of water uptake ratio in each step is carefully conducted six times at 0.5, 1, 3, 6, 12, 24, 48, 60, 72 and 84 h after GCC conduits were soaked in 10 ml of de-ionized water of pH 7.4 at room temperature. In addition, the luminal areas of the soaked GCC conduits at 24, 48, and 72 h were measured.

Cytotoxicity and Apoptosis of GCC digestion by-products

The indirect cytotoxicity was conducted in adaptation from the ISO10993-12 standard test method.[20] GCC conduits of 6 cm^2 were washed twice with sterilized 1× PBS and dried in a laminar flow. GCC digestion by-products were prepared by incubating the conduit in 1 ml of DMEM-serum free medium at 37°C for 24 h in an incubator with 75% humidity containing 5% CO_2. RSC96 Schwann cells were seeded at 1×10^4 cells/well in a 96-well tissue-culture polystyrene plate (TCPP; Corning, USA) at 37°C for 24 h in an incubator with 75% humidity containing 5% CO_2. After that, the culture medium was removed and replaced with the GCC digestion by-products (200 μL/well). After 24 h of cell incubation with the GCC digestion by-products, the solution was removed, replaced with 110 μL/well of 5 mg/ml of MTT solution in 1× PBS and further incubated in an incubator at 37°C for 4 h. Then, the MTT solution was removed and replaced with 50 μL of DMSO to dissolve the formazan. The color intensity was measured using a microplate reader (ELx800TM, Bio-Tek Instrument, Inc., Winoski, VT, USA) at the absorbance of 550 nm. Data were then expressed as a percent of control level of the optical density within an individual experiment.

Apoptotic cell death was also confirmed in the present study. After treating with the GCC digestion by-products for 48 h, the Schwann cells were washed with PBS twice, fixed in 2% paraformaldehyde for 30 min and then permeabilized with 0.1%

Triton X-100/PBS for 30 min at room temperature. After washing with PBS, TUNEL assay was performed according to the manufacturer's instructions (Boehringer Mannheim). Cells were incubated in TUNEL reaction buffer in a 37°C humidified chamber for 1 h in the dark, then rinsed twice with PBS and incubated with DAPI (1 mg/ml) at 37°C for 10 min, stained cells were visualized using a fluorescence microscope (Olympus DP70/U-RFLT50, Olympus Optical Co., Ltd., Japan). TUNEL-positive cells were counted as apoptotic cells.

Tissue Reactions to GCC Conduits

Prior to the beginning of the *in vivo* testing, the protocol was approved by the ethical committee for animal experiments of the China Medical University, Taichung, Taiwan. Transgenic mice, carrying the luciferase gene driven by NF-κB-responsive elements, were constructed as described previously.[15,16] All transgenic mice were crossed with wild-type F1 mice to yield NF-κB-luc heterozygous mice with the FVB genetic background. For insertion of the GCC implant, transgenic mice were anesthetized with 0.12 g ketamine/kg body weight and one incision (3 mm in length) on the back was made. The GCC conduit was then implanted subcutaneously into the incision and the skin was closed with silk sutures. A total of 6 transgenic mice was randomly divided into two groups of three mice: (1) sham, the incision was made and nothing

was implanted and (2) GCC, the incision was made and the GCC conduit was implanted. The mice were imaged for the luciferase activity at various time points: 1 d, 3 d, 7 d, and 28 d and subsequently sacrificed for histochemical staining. For *in vivo* imaging, mice were anesthetized with isoflurane and injected intraperitoneally with 150 mg luciferin/kg body weight. Five minutes later, mice were placed facing down in the chamber and imaged for 5 min with the camera set at the highest sensitivity by IVIS Imaging System® 200 Series (Xenogen, Hopkinton, MA). Photons emitted from tissues were quantified using Living Image® software (Xenogen, Hopkinton, MA). Signal intensity was quantified as the sum of all detected photon counts per second within the region of interest after subtracting the background luminescence and presented as photons/sec/cm^2/steradian (photons/s/cm^2/sr). For histochemical staining, the GCC implants were retrieved and fixed in 10% formalin for 2 d. Tissue was rinsed in saline and dehydrated in a series of graded alcohols (50%, 70%, and 95%) for 30 min each. Samples were then embedded in paraffin and cut into thin 12-μm sections. For histomorphometric evaluation, sections were stained with hematoxylin and eosin. The tissue reactions to the implants in the subcutaneous tissue were evaluated for uniformity and thickness of the foreign body capsule as well as the inflammation responses, such as distribution of inflammatory cells and phagocytising reaction under optical microscopy (Olympus IX70, Olympus Optical Co., Ltd., Japan).

GCC Conduits Implantation

Thirty adult Sprague-Dawley rats underwent placement of GCC conduits, which were removed upon sacrifice at various time points: 2 weeks, 5 weeks, and 8 weeks. At each implantation time, 10 rats were operated on. The animals were anesthetized with an inhalational anesthetic technique (AErrane®, Baxter, USA). Following the skin incision, fascia and muscle groups were separated using blunt dissection, and the right sciatic nerve was severed into proximal and distal segments. The proximal stump was then secured with a single 9-0 nylon suture through the epineurium and the outer wall of the GCC conduits. The distal stump was secured similarly into the other end of the chamber. Both the proximal and distal stumps were secured to a depth of 1 mm into the chamber, leaving a 10-mm gap between the stumps. The muscle layer was re-approximated with 4-0 chromic gut sutures, and the skin was closed with 2-0 silk sutures. All animals were housed in temperature (22°C) and humidity (45%) controlled rooms with 12-hour light cycles, and they had access to food and water *ad libitum*.

Electrophysiological Techniques

The animals were re-anaesthetized and their sciatic nerve exposed. The stimulating cathode was a stainless-steel monopolar needle, which was placed directly on the

sciatic nerve trunk, 5-mm proximal to the transection site. The anode was another stainless-steel monopolar needle placed 3-mm proximally to the cathode. Amplitude, latency, duration, and nerve conductive velocity (NCV) of the evoked muscle action potentials (MAP) were recorded from gastrocnemius muscles with micro-needle electrodes linked to a computer system (Biopac Systems, Inc., USA). The latency was measured from stimulus to the takeoff of the first negative deflection and the amplitude from the baseline to the maximal negative peak. The NCV was carried out by placing the recording electrodes in the gastrocnemius muscles and stimulating the sciatic nerve proximally and distally to the nerve conduit and calculated by dividing the distance between the stimulating sites by the difference in latency time. All data are expressed as mean ± standard deviation. Statistical comparisons between groups were made by the one-way analysis of variance.

Histological Processing

Immediately after the recording of muscle action potential, all of the rats were perfused transacrdially with 150 ml normal saline followed by 300 ml 4% paraformaldehtde in 0.1 M phosphate buffer, pH 7.4. After perfusion, the L4 spinal cord was quickly removed and post-fixed in the same fixative for 3-4 h. Tissue samples were placed overnight in 30% sucrose for cryoprotection at 4°C, followed by

embedding in optimal cutting temperature solution. Samples were the kept at -20°C until preparation of 18 μm sections was performed using a cryostat, with samples placed upon poly-L-lysine-coated slide. Immunohistochemistry of frozen sections was carried out using a two-step protocol according to the manufacturer's instructions (Novolink Polymer Detection System, Novocastra). Briefly, endogenous peroxidase activity in frozen sections was inactivated with incubation of the slides in 0.3% H_2O_2, and nonspecific binding sites were blocked with Protein Block (RE7102; Novocastra). After serial incubation with rabbit- anti-CGRP polyclonal antibody 1:1000 (calbiochem, Germany), Post Primary Block (RE7111; Novocastra), and secondary antibody (Novolink Polymer RE7112), the sections were developed in diaminobenzidine solution under a microscope and counterstained with hematoxylin. Sciatic nerve sections were taken from the middle regions of the regenerated nerve in the chamber. After the fixation, the nerve tissue was post-fixed in 0.5% osmium tetroxide, dehydrated, and embedded in spurs. The tissue was then cut to 5-µm thickness by using a microtome with a dry glass knife, stained with toluidine blue.

Image Analysis

All tissue samples were observed under optical microscopy. CGRP-immunoreactivity (IR) in dorsal and ventral horns in the lumbar spinal cord was detected by

immunohistochemistry as described previously.[21] The immuno-products were confirmed positive-labeled if their density level was over five times background levels. Under a 100x magnification, the ratio of area occupied by positive CGRP-IR in the dorsal horn and CGRP-expressing cells in the ventral horn following neurorrhaphy relative to the lumbar spinal cord bilaterally was measured using an image analyzer system (Image-Pro Lite, Media Cybernetics, USA) coupled to the microscope. Statistical comparisons between groups at different time points post-surgery were made by the one-way analysis of variance. Student's t-test was used to compare the bilateral CGRP-IR differences at the same time point.

As counting the myelinated axons, at least 30 to 50 percent of the sciatic nerve section area randomly selected from each nerve specimen at a magnification of 400x was observed. The axon counts were extrapolated by using the area algorithm to estimate the total number of axons for each nerve. Axon density was then obtained by dividing the axon counts by the total nerve areas. Statistical comparisons between groups were made by the one-way analysis of variance.

Results and Discussion

Macroscopic Observation of GCC Conduits

GCC conduits were brownish in appearance caused by the reaction between

glutaraldehyde and amino acids or proteins. Figure 2 shows the GCC conduit was concentric and round with a smooth inner lumen and outer wall surface.

Physical Characteristics of GCC Conduits

The cross-linking index of GCC conduits, expressed as a percentage of free amino groups lost during cross-linking, was 77.1 ± 0.7%. It means that 1.0 wt.% glutaraldehyde was sufficient to cross-link about 77.1% of the amino groups. The maximum tensile strength and the water contact angle of GCC conduits were 44.2±4.7 MPa and 58.4±6.9 degree. Compared to the biodegradable materials reported in the literature (Table 1), the GCC had a relatively larger maximum tensile strength at 44.2± 4.7 MPa which should have sufficient tensile strength to be utilized as a nerve graft when compared to the tensile strength of fresh rat sciatic nerve (2.72±0.97 MPa) reported by Borschel et al.[32] In addition, the water contact angle of the GCC was 58.4±6.9 degree which was hydrophilic that should be conducive to cell adhesion and growth. Figure 3 represents the water uptake ratios of the soaked GCC conduits. In the first 6 hr, the weight uptake of the GCC conduits increased markedly. A tendency for attenuated water uptake was observed which was almost at a plateau when the soaking period exceeded 6 h. Similarly, the luminal areas of the GCC conduits were increased dramatically (Table 2). However, all of the GCC conduits still maintained

the lumens and wall integrity even after 80 h of soaking, indicating that the glutaraldehyde cross-linked casein matrix provided a framework with high mechanical strength.

Cytotoxicity and Apoptosis of GCC Conduits

Spindle-shaped cellular morphology of Schwann cells cultured on the culture plate was viable and there was no sign of infection. The color of DMEM with the digestion products of the GCC conduits after 24 h became yellowish. Treatment with the GCC digestion by-products did not induce apoptotic cell death since only very few TUNEL positive cells were seen, suggesting that the DNA fragmentation did not occur in these Schwann cells (Fig. 4A). This result was supported by the cytotoxic test that the optical density of the Schwann cells was not significantly different as compared to that of the controls after exposing to the GCC digestion by-products (Fig. 4B), indicating that these conduits would not induce cytotoxic effects to the cultured cells.

Tissue Reactions to GCC Conduits

No intense foreign-body reactions or necrosis of tissues were seen for any of the rats in the postoperative period. The GCC implant was implanted subcutaneously on the back of the mice and the NF-κB-driven bioluminescent signals were monitored by

luminescent imaging on the indicated periods (Fig. 5A). As a result, luminescent signal in the implanted region was initially increased and dramatically decreased (Fig. 5B). NF-κB activity reached a maximal activation at 3 d where a strong and specific in vivo bioluminescence around the implantation site was observed. In consistent with the bioluminescent signals, an acute inflammatory response was characterized by a rapid accumulation of cells resembling lymphocytes and macrophages at the site between GCCs and their surrounding tissue at 1 d post-implantation (Fig. 6A). GCCs still persisted maintaining their lumens and wall integrity at this time point. At 3 d, a delicate fibrous tissue capsule with dispersing neocapillaries was present surrounding the whole implant. Inflammation responses were still obvious with abundant inflammatory cells (Fig. 6B). Phagocytising reaction became obvious at the interfaces between the GCC materials and tissues after 7 d of implantation (Fig. 6C). At the time points of 28 d, fibrous tissue capsules became thicker with a compact structure along with active neovascularization. Up to this time, inflammatory reaction continued with macrophages digesting the fragmented GCC materials (Fig. 6D).

Electrophysiological Measurements

MAPs were recorded at postoperative intervals of 2, 5, and 8 weeks. All of the electrophysiological indexes, including amplitude, latency, duration, and NCV of the

regenerated nerves were improved as a function of the experimental period (Fig. 7A-7D). Specifically, the regenerated nerves at 8 weeks postoperatively had a significantly shorter latency and larger duration, amplitude and NCV as compared to those at 2 and 5 weeks of recovery.

CGRP-IR in the Spinal Cord

Immunohistochemical staining showed that CGRP-labeled fibers were noted in the area of lamina III-V (Fig. 8). Lamina I-II regions in the dorsal horn of the lumbar spinal cord bilaterally were strongly CGRP-immunolabeled on week 2, and then notably decreased on weeks 5 to 8 (Fig. 9A-9B). In addition, CGRP-expressing cells in the ventral horns of the lumbar spinal cord bilaterally displayed the typical morphological characteristics of motoneurons (Fig. 9C-9D). Specifically, the ratio of area occupied by positive CGRP-IR ipsilateral to the injury was significantly decreased on week 8 compared to that on week 2 post-surgery (Fig. 10A-10B). Similarly, the CGRP-expressing cell numbers in the ventral horns peaked on week 2 post-injury, and dramatically declined from weeks 5 to 8 (Fig. 10C-10D). It was noted that the CGRP-IR area ratios and the CGRP-expressing cell numbers ipsilateral to the injury were all relatively larger than those from contralateral IR at the three different time point post-surgery (Fig. 11A-11B). Specifically, the bilateral differences in

CGRP-IR area ratios on week 2 and CGRP-expressing cell numbers on weeks 2 and 5 differed significantly. These results indicated CGRP expression differed depending upon the location in the lumbar spinal cord and the recovery stage of regenerating sciatic nerve in the GCC conduit.

Sciatic Nerve Regeneration

Throughout the 8 weeks of experimental period, no nerve dislocation out of the GCC conduits was seen for all of the rats. Brownish fibrous tissue encapsulation was noted, covering all over the GCC conduits. After trimming the fibrous tissue, cutting the wall of the tube, the regenerated nerve was exposed and then retrieved. Observing the muscle tissue surrounding the conduit, no obvious inflammation or adhesion was found. Overall gross examination of the GCC conduits at the three observation time points all revealed 100% of nerve formation in the tubes.

At 2 weeks post-implantation, swelling or deformation of the GCCs was not seen. Regenerated nerves in the GCCs were still immature composed of fibrin matrices, which were populated by Schwann cells and blood vessels (Fig. 12A). At this stage, it is difficult to discriminate between the endoneurial areas and their surrounding fibrous tissues.

At 5 weeks, the GCCs featured a partially fenestrated outer layer; however, they

still remained circular with a round lumen. Up to this time, the regenerated nerves became more mature, displaying a structure with a symmetric epineurium, surrounding a cellular and vascularized endoneurium in which numerous myelinated axons had been seen (Fig. 12B).

At 8 weeks, fragmentation of the GCCs continued but their architecture still remained. As seen at 5 weeks of regeneration, the nerves at this stage had a mature structure with a large number of myelinated axons interposed in the endoneurium with rich neovascularization (Fig. 12C).

By comparison, the nerve maturity and the spatial temporal progression of cellular activity within the GCC conduits are similar to those seen in the silicone rubber conduits.[33]

Morphometric Measurements

As aforementioned results, nerve features in the GCC conduits at 2 weeks of implantation were too immature to be included in comparisons of their morphometric measurements. By comparison, morphometric studies revealed available data in regenerated nerves in both the tube groups after 5 and 8 weeks of implantation. No significant difference was seen between the mean values of their myelinated axon number, axon area, axon density, and total nerve area (Fig. 13A-13D).

General Discussion

Peripheral nerve injuries are very common in clinical practice. Nowadays, autologous nerve grafting is the most commonly used technique to reconstruct the peripheral nerve defect. However, grafting has a number of inevitable disadvantages including morbidity at the donor site and limited supply of donor nerves.[34,35] Though nerve allografts may be used to overcome these problems, few successes were achieved due to the immunological rejection.[36,37] Therefore, the use of an artificial guide for reconstruction of nerve gaps can be seen as an alternative. In recent years, enormous efforts in clinical and experimental investigations have been made to seek proper biomaterials to fabricate the artificial guides, such as silicone rubber,[38,39] collagen,[40,41] gelatin,[42,43] polylactates,[25,44] polycaprolactone,[45] and so on. In this study, for the first time, we proved that the casein crosslinked by glutaraldehyde was suitable for application as artificial nerve conduits.

Due to its excellent mechanical properties, the glutaraldehyde-crosslinked casein conduits were successfully prepared. The GCC conduits had uniform and compact wall microstructures which could prevent the connective and scar tissues from growing into the internal lumen to hinder the nerve regeneration. In addition, the GCC did not induce cytotoxic effects to the cultured Schwann cells, which had a good hydrophilicity and could keep its integrity even after 80 h of soaking in the de-ionized

water. The noninvasive real-time NF-κB bioluminescence imaging accompanied with histochemical assessment also showed the GCC was highly biocompatible, only evoking a mild tissue response. These results are not surprising since the casein has been shown a promising material for use in drug delivery,[46] and the glutaraldehyde shown prominent cross-linking capability for artificial organs including bones, corneas, skins, and nerves.[47-50]

From *in vivo* observations, we found the GCC conduits did not display any unsatisfactory swelling or deformation during the long *in vivo* implant period after surgery. The stable dimensions of the GCC conduits could result from the chemical crosslinking of glutaraldehyde with the amino groups on the casein macromolecular chains.[51] Healthy growth of nerve tissues was observed in all conduits, again confirming the good biocompatibility of GCC to nerve tissues. MAPs are thought to reappear when regenerating myelinated nerve fibers have reached their target organ.[52-54] The electrophysiological indexes, including amplitude, latency, duration, and NCV of the regenerated nerves were improved as a function of the experimental period which could be attributed to the quick recovery of nerve conducting function in the implanted rats. In addition, histological assessment showed that the temporal and spatial progresses of cellular activity within the GCC conduits are similar to those seen for experiments using artificial guides for peripheral nerve regeneration reported

in the literature.[33,55] At 2 weeks post-surgery, fibrin matrices had formed in the GCC conduits, providing a framework for subsequent migration of fibroblasts, Schwann cells, and axons from the severed ends. After 5 weeks of regeneration, myelinated axons had grown across the gap, indicating the GCC conduit could offer a beneficial environment to the growing axons. These histological results were supported by the protein levels of CGRP in associated spinal cord segments, which were gradually decreased during the test period. Since the CGRP has been recognized as a nerve regeneration-promoting peptide *in vivo*,[56-58] it can therefore be surmised that when regenerating nerves becomes more mature, the CGRP expression in the spines may decline and return to normal values as a consequence of reconnection of the two severed nerve stumps.

Finally, the quantitative data in several recent studies on biodegradable bridging conduits to repair injured rat sciatic nerves were gleaned from the literature. It is noted that the quantitative data in the regenerated nerves in the GCC conduits (myelinated axon density = 28,000/mm^2) are about in the same range or even better than those in most of the biodegradable conduits, such as the chitosan (15,300/mm^2),[59] the polylactic acid (mostly unmyelinated axons),[3] the polyglycolic acid (15,300/mm^2),[60] the collagen (38,100/mm^2),[61] the proanthocyanidin cross-linked gelatin (mostly unmyelinated axons),[62] and the genipin cross-linked

gelatin (mostly unmyelinated axons).[62] In addition, the temporal and spatial progresses of cellular activity within the GCC conduit are similar to those seen for experiments using silicone rubber nerve guides,[42,63] which have largely been used in clinical practice. These results show the casein crosslinked by glutaraldehyde could be a potential material for application as artificial nerve conduits.

Conclusion

The current study is the first work dedicated to GCC, a newly devised biodegradable nerve bridge. Combined with the superior properties including strong mechanical microstructure, high biocompatibility, no toxicity, as well as good applicability for nerve regeneration together with excellent electrophysiological progress, the casein based conduits can be effectively used for peripheral nerve damage repair.

Acknowledgements

This research is supported in part by China Medical University and Hospital (CMU99-EW-03; DMR99-075) and Taiwan Department of Health Clinical Trial and Research Center of Excellence (DOH100-TD-B-111-004). We also would like to thank Dr. Tin-Yun Ho for the experimental help.

Captions

Table 1: Maximum tensile strength and water contact angle of nerve bridging materials reported in the literature.

Table 2: Luminal areas of the soaked GCC conduits.

Figure 1: Schematic drawing of the dumbbell-shaped sample used in the mechanical testing (not for real scale).

Figure 2: SEM micrograph of the GCC conduit.

Figure 3: Time effect on the water uptake ratio of soaked GCC conduits.

Figure 4: Induction of apoptosis and cytoxicity by soaking solution of GCC conduits. (A) Nuclei of Schwann cells were characterized by DAPI and TUNEL assay and investigated under a fluorescent microscopy. (B) Quantification of cytotoxic test of soaking solutions of GCC conduits relative to the controls on Schwann cells. Values are mean±standard error.

Figure 5: NF-κB-dependent bioluminescence in living mice implanted with GCC conduits. (A) Diagrams show the bioluminescent signal within a radius of 2.5 mm of implanted region (boxed area). The color overlay on the image represents the photons/s emitted from the animal, as indicated by the color scales. (B) Quantification of photon emission within the implanted region. Values are mean±standard error of three mice.

Figure 6: Micrograph of interface area between the host and GCC conduits implanted for (A) 1 d, (B) 3 d, (C) 7d, and (D) 28 d. Note a rapid accumulation of inflammatory cells (arrows) phagocytising the disintegrated GCC materials. Fibrous tissue capsules (FTC) were thick with a compact structure at 28 d after implantation. Scale bars = 100 μm.

Figure 7: Analysis of the evoked muscle action potentials, including (A) peak amplitude, (B) latency, and (C) NCV. *P<0.05, significant difference from other examined time points.

Figure 8: CGRP-IR in the lumbar spinal cord after injury. (A) The area of lamina III-V examined for CGRP-labeled fibers (arrows). Shown in (B) is the higher magnification of the boxed area in (A). Scale bars = 100 μm for panel A, 25 μm for for panel B.

Figure 9: CGRP-IR in the (A) dorsal horn ipsilateral to the injury, (B) dorsal horn contralateral to the injury. CGRP-expressing cells (arrows) in the (C) ventral horn ipsilateral to the injury, (D) ventral horn contralateral to the injury. Scale bars = 100 μm

Figure 10: Comparisons of CGRP-IR area ratios at different time points post-surgery in the (A) dorsal horns ipsilateral to the injury (B) dorsal horn contralateral to the injury and CGRP-expressing cell numbers in the (C) ventral horn

ipsilateral to the injury, (D) ventral horn contralateral to the injury. *P<0.05, significant difference from other examined time points.

Figure 11: Comparisons of (A) CGRP-IR area ratios at the same time point post-surgery between the dorsal horns and (B) CGRP-expressing cells between the ventral horns. *P<0.05, significant difference from other examined locations.

Figure 12: Light micrographs of regenerated nerve cross-sections at different implantation periods, (A) 2 weeks, (B) 5 weeks, and (C) 8 weeks. At 2 weeks, regenerated nerves were only composed of fibrin matrices populated by Schwann cells (SC). After 5 weeks, myelinated (MA) and unmyelinated axons (UA) had been seen in the endoneurium (ED) surrounded by the epineurium (EP). Scale bars = 100 μm.

Figure 13: Morphometric analysis from the regenerated nerves in the GCC conduits, including (A) axon number, (B) axon area, (C) axon density, and (D) total nerve area. *P<0.05, significant difference from other examined time points.

References

[1] C. C. Yeh, Y. C. Lin, F. J. Tsai, C. Y. Huang, C. H. Yao, Y. S. Chen, *Neurorehabil. Neural Repair* **2010**, *24*, 730.

[2] M. C. Lu, C. H. Yao, S. H. Wang, Y. L. Lai, C. C. Tsai, Y. S. Chen, *J. Trauma* **2010**, *68*, 434.

[3] M. C. Lu, C. C. Tsai, S. C. Chen, F. J. Tsai, C. H. Yao, Y. S. Chen, *J. Trauma* **2009**, *67*, 1066.

[4] J. Y. Chang, T. Y. Ho, H. C. Lee, Y. L. Lai, M. C. Lu, C. H. Yao, Y. S. Chen, *Artif. Organs* **2009**, *33*, 1075.

[5] P. Plikk, S. Målberg, A. C. Albertsson, *Biomacromolecules* **2009**, *10*, 1259.

[6] L. Thomsen, P. Bellemere, T. Loubersac, E. Gaisne, P. Poirier, F. Chaise, *Chir. Main.* **2010**, *29*, 255.

[7] M. Merle, A. L. Dellon, J. N. Campbell, P. S. Chang, *Microsurgery* **1989**, *10*, 130.

[8] R. Birch, *Hand* **1979**, *11*, 211.

[9] I. V. Yannas, B. J. Hill, *Biomaterials* **2004**, *25*, 1593.

[10] W. N. Eigel, C. J. Hofmann, B. A. Chibber, J. M. Tomich, T. W. Keenan, E. T. Mertz, *Proc. Natl. Acad. Sci. U.S.A.* **1979**, *76*, 2244.

[11] W. R. Aimutis, E. T. Kornegay, W. N. Eigel, *J. Dairy Sci.* **1982**, *65*, 1874.

[12] G. F. Chi, M. R. Kim, D. W. Kim, M. H. Jiang, Y. Son, *Exp. Neurol.* **2010**, *222*, 304.

[13] H. Liu, Y. Kim, S. Chattopadhyay, I. Shubayev, J. Dolkas, V. I. Shubayev, *J.*

Neuropathol. Exp. Neurol. **2010**, *69*, 386.

[14] J. Wang, P. Zhang, Y. Wang, Y. Kou, H. Zhang, B. Jiang, *Artif. Cells Blood Substit. Immobil. Biotechnol.* **2010**, *38*, 24.

[15] T. Y. Ho, Y. S. Chen, C. Y. Hsiang, *Biomaterials* **2007**, *28*, 4370.

[16] C. Y. Hsiang, Y. S. Chen, T. Y. Ho, *Biomaterials* **2009**, *30*, 3042.

[17] A. Loesch, H. Tang, M. A. Cotter, N. E. Cameron, *Angiology* **2010**, *61*, 651.

[18] E. Adeghate, H. Rashed, S. Rajbandari, J. Singh, *Ann. N. Y. Acad. Sci.* **2006**, *1084*, 296.

[19] X. Q. Li, V. M. Verge, J. M. Johnston, D. W. Zochodne, *J. Neuropathol. Exp. Neurol.* **2004**, *63*, 1092.

[20] International Standard ISO10993-5, *Biological Evaluation of Medical Devices. Part 5: Tests for Cytotoxicity: In Vitro Methods* 1992.

[21] L. F. Zheng, R. Wang, Y. Z. Xu, X. N. Yi, J. W. Zhang, Z. C. Zeng, *Brain Res.* **2008**, *1187*, 20.

[22] X. Wang, L. Sang, D. Luo, X. Li, *Colloids Surf. B Biointerfaces* **2011**, *82*, 233.

[23] A. Sionkowska, J. Skopinska-Wisniewska, M. Gawron, J. Kozlowska, A. Planecka, *Int. J. Biol. Macromol.* **2010**, *47*, 570.

[24] C. Huang, R. Chen, Q. Ke, Y. Morsi, K. Zhang, X. Mo, *Colloids Surf. B Biointerfaces* **2011**, *82*, 307.

[25] M. Sun, S. Downes, *J. Mater. Sci. Mater. Med.* **2009**, *20*, 1181.

[26] W. Wang, S. Itoh, A. Matsuda, S. Ichinose, K. Shinomiya, Y. Hata, J. Tanaka, *J. Biomed. Mater. Res. A* **2008**, *84*, 557.

[27] M. F. Meek, K. Jansen, R. Steendam, W. van Oeveren, P. B. van Wachem, M. J. van Luyn, *J. Biomed. Mater. Res. A* **2004**, *68*, 43.

[28] B. A. Harley, J. H. Leung, E. C. Silva, L. J. Gibson, *Acta Biomater.* **2007**, *3*, 463.

[29] M. P. Prabhakaran, J. R. Venugopal, S. Ramakrishna, *Biomaterials* **2009**, *30*, 4996.

[30] L. Ghasemi-Mobarakeh, M. P. Prabhakaran, M. Morshed, M. H. Nasr-Esfahani, S. Ramakrishna, *Biomaterials* **2008**, *29*, 4532.

[31] J. Pan, M. Zhao, Y. Liu, B. Wang, L. Mi, L. Yang, *J. Biomed. Mater. Res. A* **2009**, *89*, 160.

[32] G. H. Borschel, K. F. Kia, W. M. Kuzon, R. G. Dennis, *J. Surg. Res.* **2003**, *114*, 133.

[33] L. R. Williams, F. M. Longo, H. C. Powell, G. Lundborg, S. Varon, *J. Comp. Neurol.* **1983**, *218*, 460.

[34] P. G. di Summa, P. J. Kingham, W. Raffoul, M. Wiberg, G. Terenghi, D. F. Kalbermatten, *J. Plast. Reconstr. Aesthet. Surg.* **2010**, *63*, 1544.

[35] T. Matsuyama, M. Mackay, R. Midha, *Neurol. Med. Chir. (Tokyo)* **2000**, *40*, 187.

[36] M. Rivlin, E. Sheikh, R. Isaac, P. K. Beredjiklian, *Hand Clin.* **2010**, *26*, 435.

[37] A. Klimczak, M. Siemionow, *Semin. Plast. Surg.* **2007**, *21*, 226.

[38] M. D. Wood, D. Hunter, S. E. Mackinnon, S. E. Sakiyama-Elbert, *J. Biomater. Sci. Polym. Ed.* **2010**, *21*, 771.

[39] M. Ishiguro, K. Ikeda, K. Tomita, *J. Orthop. Sci.* **2010**, *15*, 233.

[40] S. Madduri, P. di Summa, M. Papaloïzos, D. Kalbermatten, B. Gander, *Biomaterials* **2010**, *31*, 8402.

[41] L. Yao, G. C. de Ruiter, H. Wang, A. M. Knight, R. J. Spinner, M. J. Yaszemski, A. J. Windebank, A. Pandit, *Biomaterials* **2010**, *31*, 5789.

[42] Y. C. Yang, C. C. Shen, T. B. Huang, S. H. Chang, H. C. Cheng, B. S. Liu, *J. Biomed. Mater. Res. B Appl. Biomater.* **2010**, *95*, 207.

[43] C. J. Chang, *J. Biomed. Mater. Res. A* **2009**, *91*, 586.

[44] H. B. Wang, M. E. Mullins, J. M. Cregg, C. W. McCarthy, R. J. Gilbert, *Acta Biomater.* **2010**, *6*, 2970.

[45] C. M. Valmikinathan, S. Defroda, X. Yu, *Biomacromolecules* **2009**, *10*, 1084.

[46] A. J. Santinho, J. M. Ueta, O. Freitas, N. L. Pereira, *J. Microencapsul.* **2002**, *19*, 549.

[47] M. B. Keogh, F. J. O'Brien, J. S. Daly, *Acta Biomater.* **2010**, *6*, 4305.

[48] E. Bentley, C. J. Murphy, F. Li, D. J. Carlsson, M. Griffith, *Cornea* **2010**, *29*,

910.

[49] M. B. Dainiak, I. U. Allan, I. N. Savina, L. Cornelio, E. S. James, S. L. James, S. V. Mikhalovsky, H. Jungvid, I. Y. Galaev, *Biomaterials* **2010**, *31*, 67.

[50] M. H. Chen, P. R. Chen, M. H. Chen, S. T. Hsieh, J. S. Huang, F. H. Lin, *J. Biomed. Mater. Res. B* **2006**, *77*, 89.

[51] M. S. Latha, A. V. Lal, T. V. Kumary, R. Sreekumar, A. Jayakrishnan, *Contraception* **2000**, *61*, 329.

[52] F. Werdin, H. Grüssinger, P. Jaminet, A. Kraus, T. Manoli, T. Danker, E. Guenther, M. Haerlec, H. E. Schaller, N. Sinis, *J. Neurosci. Methods* **2009**, *182*, 71.

[53] N. Lago, F. J. Rodríguez, M. S. Guzmán, J. Jaramillo, X. Navarro, *J. Neurosci. Res.* **2007**, *85*, 2800.

[54] H. Y. Chiang, H. F. Chien, H. H. Shen, J. D. Yang, Y. H. Chen, J. H. Chen, S. T. Hsieh, *J. Neuropathol. Exp. Neurol.* **2005**, *64*, 576.

[55] M. C. Lu, C. Y. Ho, S. F. Hsu, H. C. Lee, J. H. Lin, C. H. Yao, Y. S. Chen, *Neurorehabil. Neural Repair* **2008**, *22*, 367.

[56] I. A. Belyantseva, G. R. Lewin, *Eur. J. Neurosci.* **1999**, *11*, 457.

[57] A. Blesch, M. H. Tuszynski, *J. Comp. Neurol.* **2001**, *436*, 399.

[58] L. J. Chen, F. G. Zhang, J. Li, H. X. Song, L. B. Zhou, B. C. Yao, F. Li, W. C. Li, *J. Clin. Neurosci.* **2010**, *17*, 87.

[59] G. Wang, G. Lu, Q. Ao, Y. Gong, X. Zhang, *Biotechnol. Lett.* **2010**, *32*, 59.

[60] T. Waitayawinyu, D. M. Parisi, B. Miller, S. Luria, H. J. Morton, S. H. Chin, T. E. Trumble, *J. Hand Surg. Am.* **2007**, *32*, 1521.

[61] B. S. Liu, *J. Biomed. Mater. Res. A* **2008**, *87*, 1092.

[62] Y. S. Chen, J. Y. Chang, C. Y. Cheng, F. J. Tsai, C. H. Yao, B. S. Liu, *Biomaterials* **2005**, *26*, 3911.

[63] F. Xie, Q. F. Li, B. Gu, K. Liu, G. X. Shen, *Microsurgery* **2008**, *28*, 471.

Table 1

Materials	Maximum tensile strength	Water contact angle
(1) collagen-chitosan[22]	248.2 to 361.2 kPa	N/A
(2) collagen crosslinked by EDC/NHS[23]	77.9 to 92.5 MPa	44.1° to 74.9°
(3) collagen-chitosan-polyurethane[24]	9.38 MPa	N/A
(4) poly - ε -caprolactone[25]	10.73 to 16.3 MPa	36.7° to 80.03°
(5) chitosan[26]	0.64 MPa	N/A
(6) poly(DL-lactide- ε -caprolactone)[27]	13 MPa	N/A
(7) collagen-glycosaminoglycan[28]	2.0 kPa	N/A
(8) poly(L-lactic acid)-co-poly-(ε -caprolactone)/ collagen[29]	4.61 MPa	57°
(9) poly(ε -caprolactone)/ gelatin[30]	0.8 MPa	32°
(10) poly(ethylene glycol)-graft-poly(D,L-lactic acid)[31]	N/A	50.4°

Table 2

Soaking time (hr)	0	24	48	72
Luminal area (mm^2)	66.0±3.8	125.9±8.6	166.6±7.5	187.6±7.2

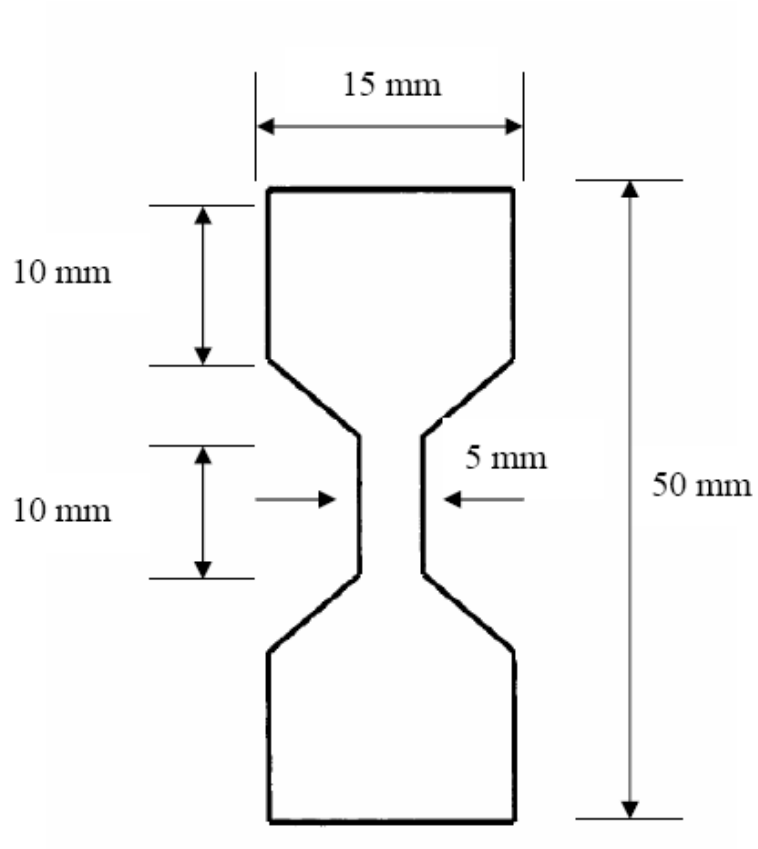

Figure 1

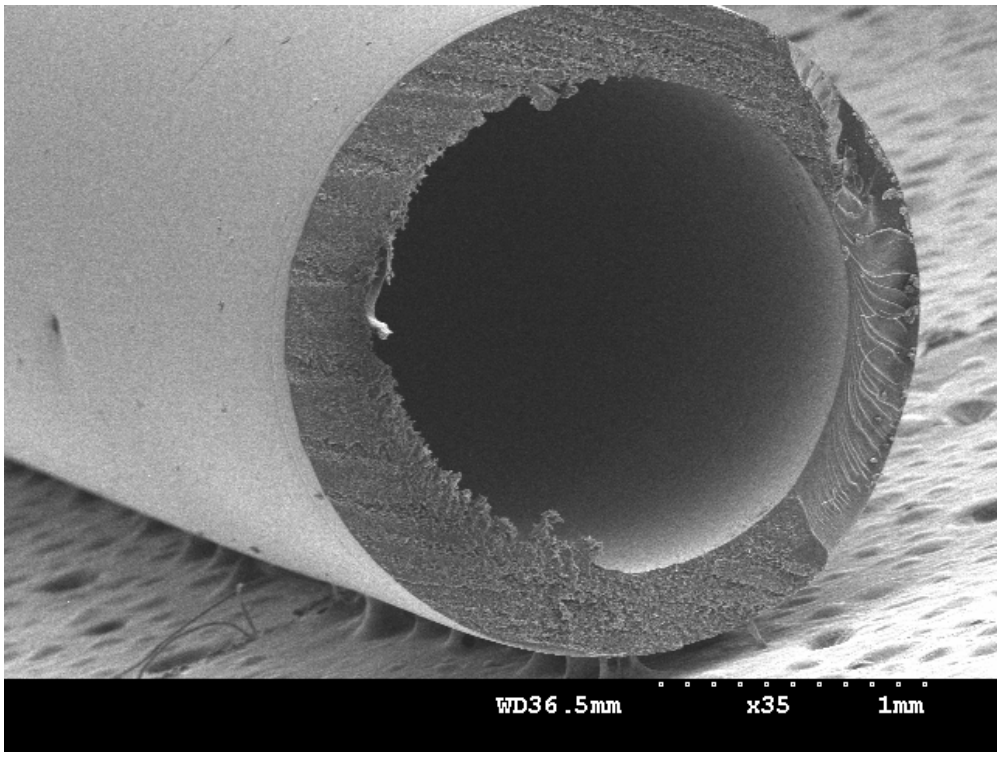

Figure 2

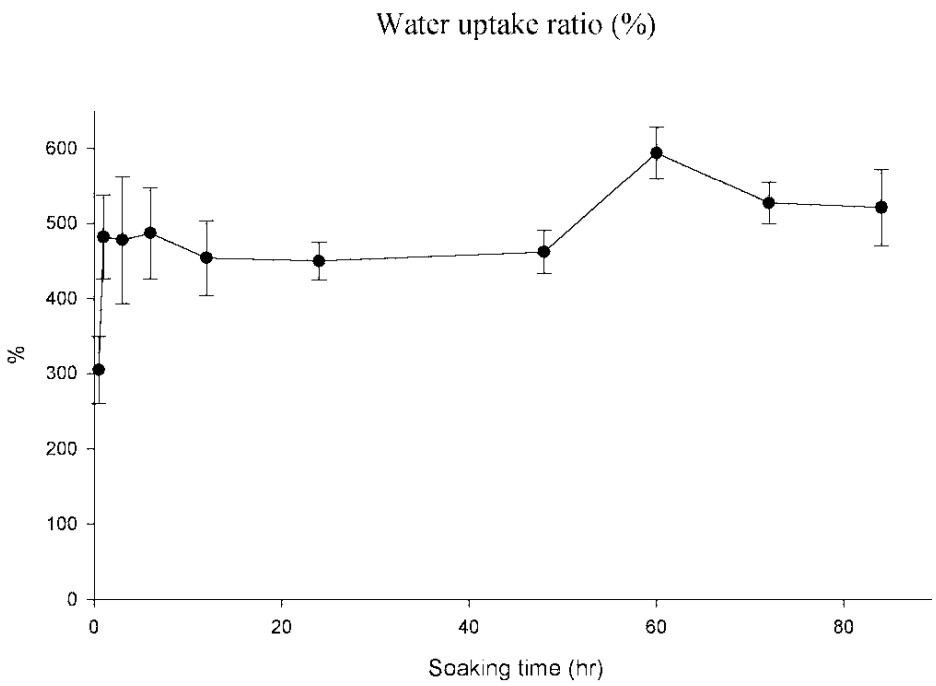
Water uptake ratio (%)
600
500
400
300
200
100
0
%
0
20
40
60
80
Soaking time (hr)

Figure 3

(A)

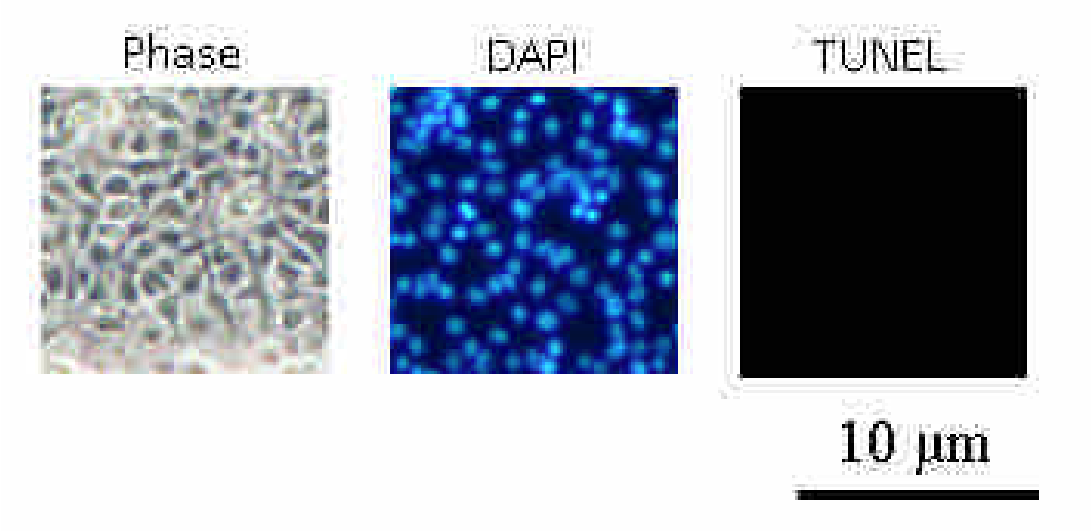
Phase
DAPI
TUNEL
10 μm

(B)

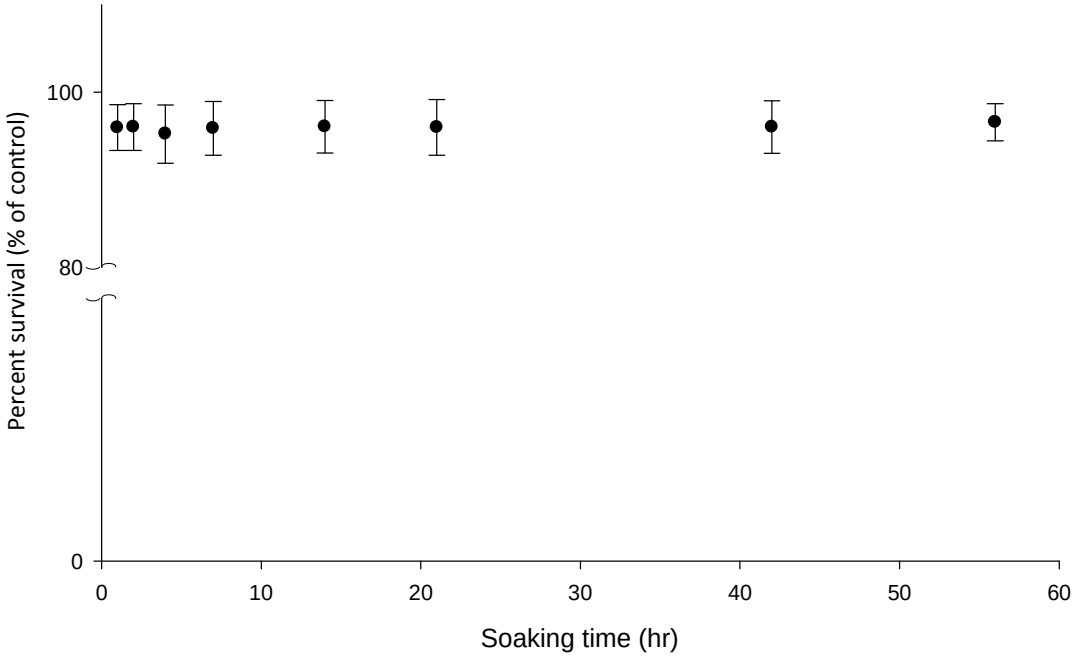
Percent survival (% of control)
100
80
0
0
10
20
30
40
50
60
Soaking time (hr)

Figure 4

(A)

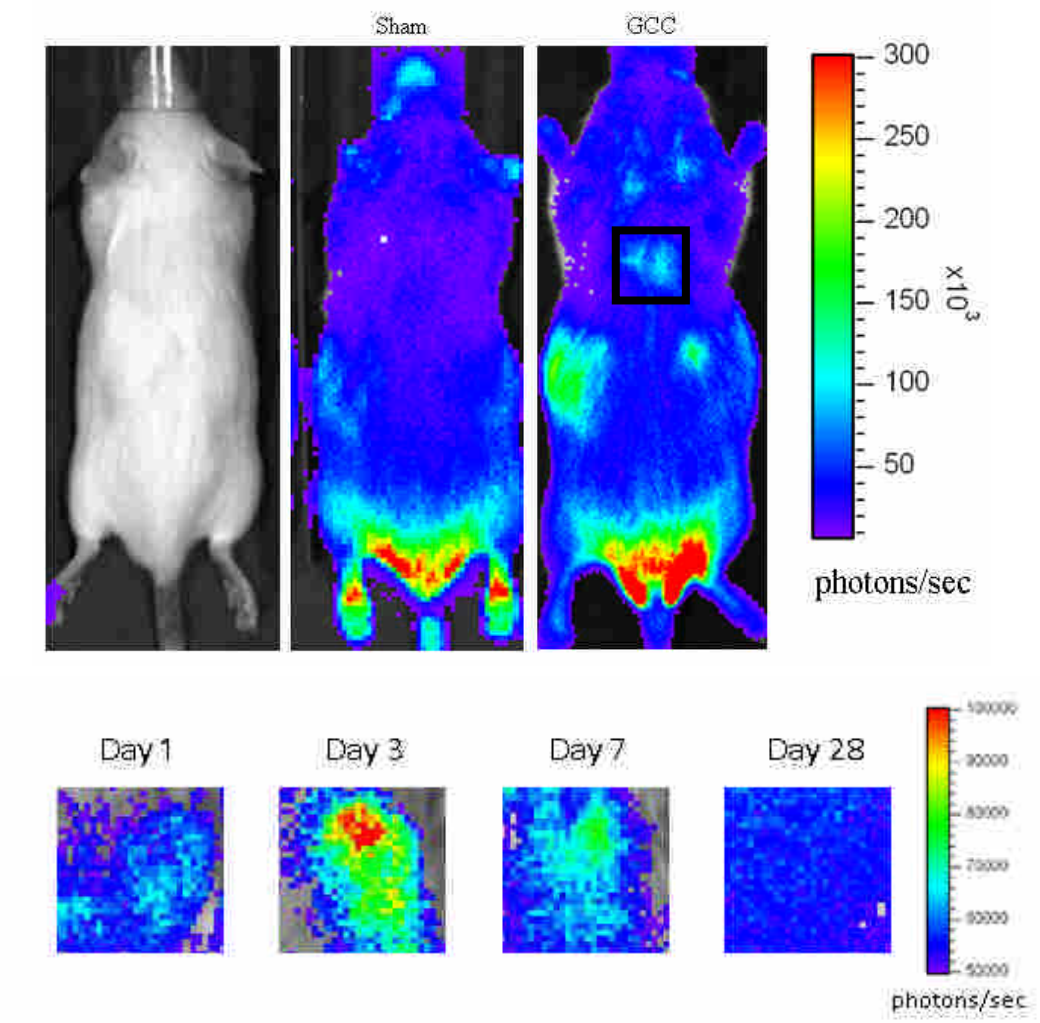
Sham
GCC
300
250
200
150
100
50
x10³
photons/sec
Day 1
Day 3
Day 7
Day 28
photons/sec

(B)

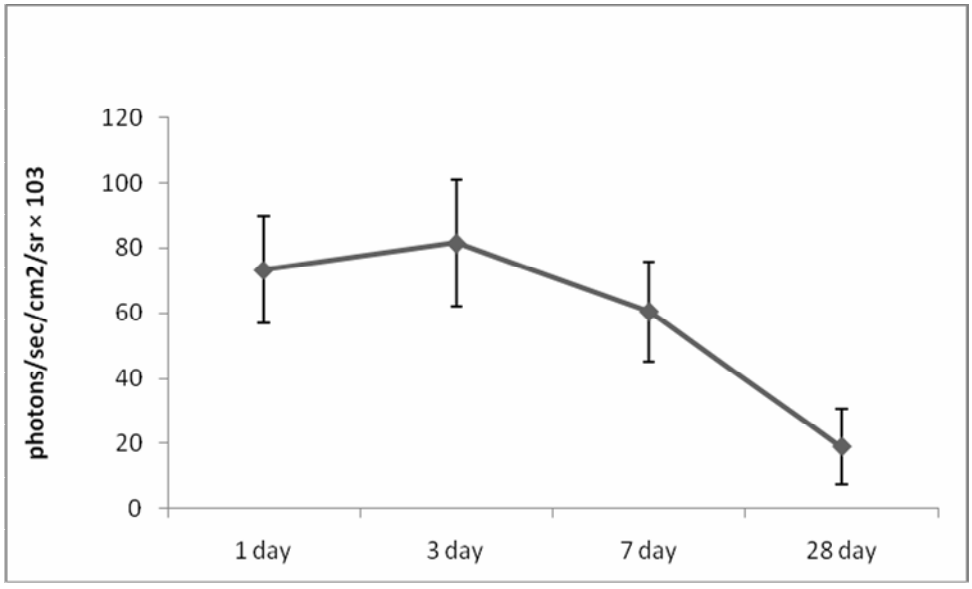
photons/sec/cm2/sr × 103
120
100
80
60
40
20
0
1 day
3 day
7 day
28 day

Figure 5

(A)

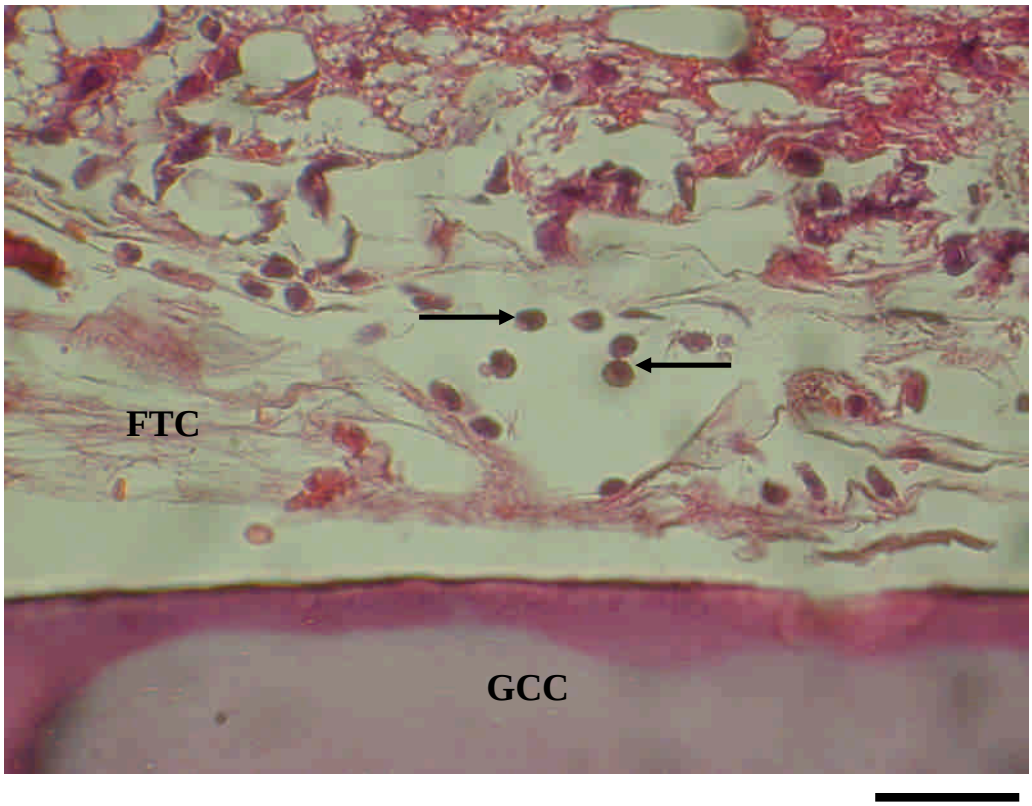

(B)

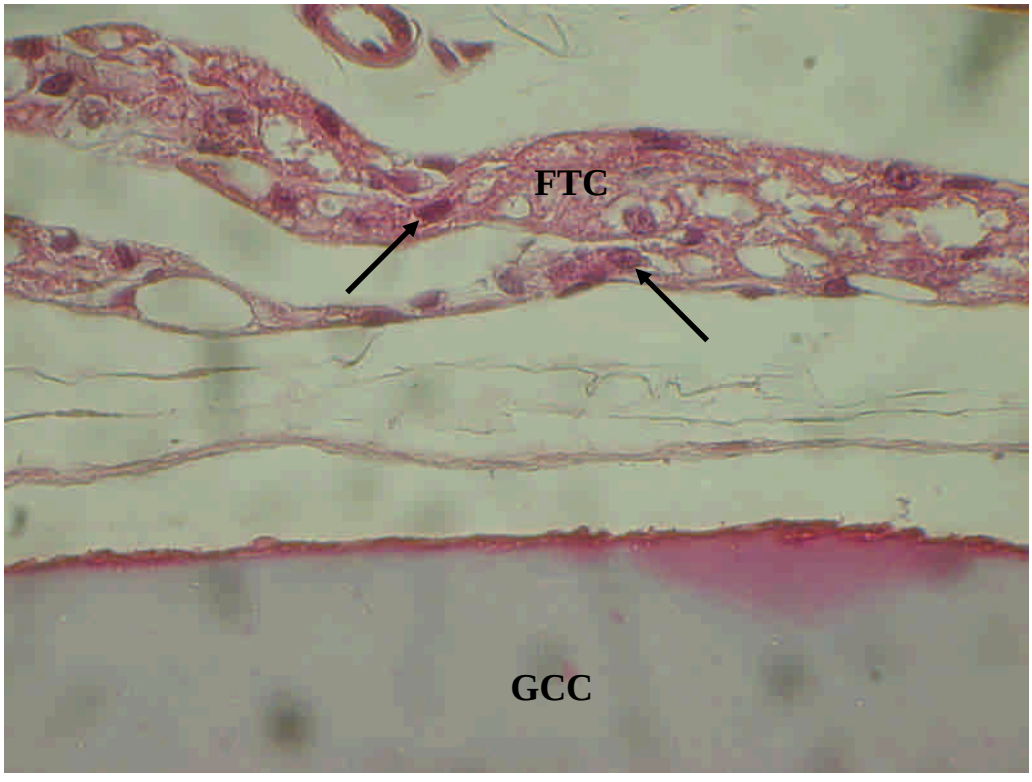

(C)

(D)

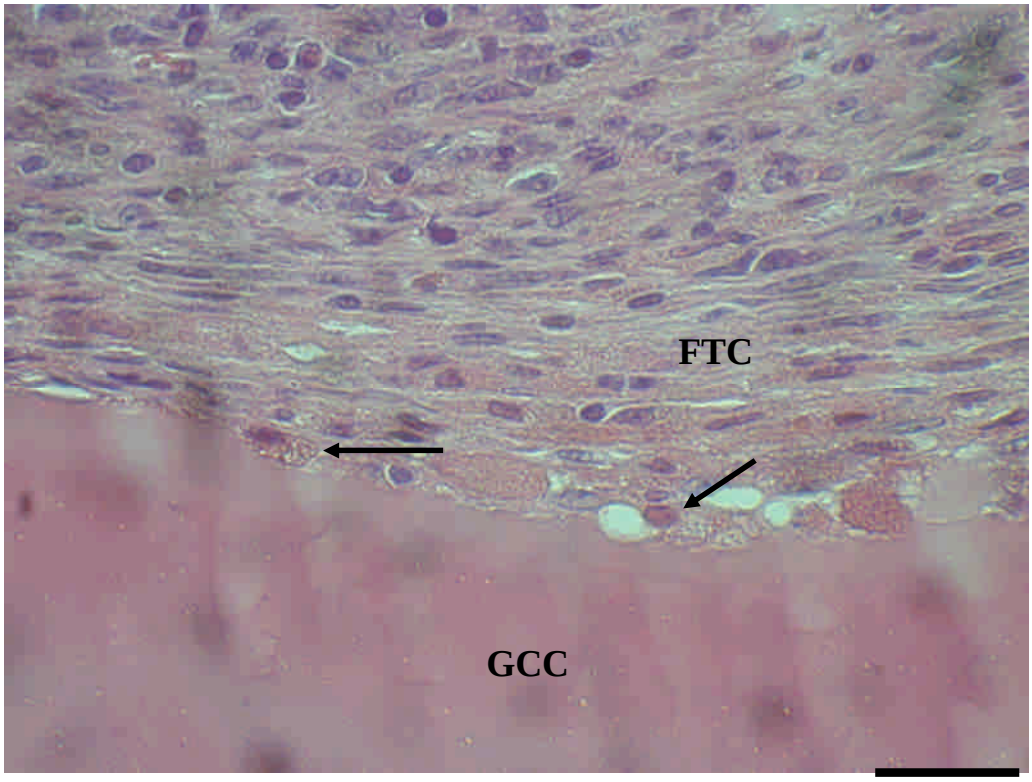

Figure 6

(A)

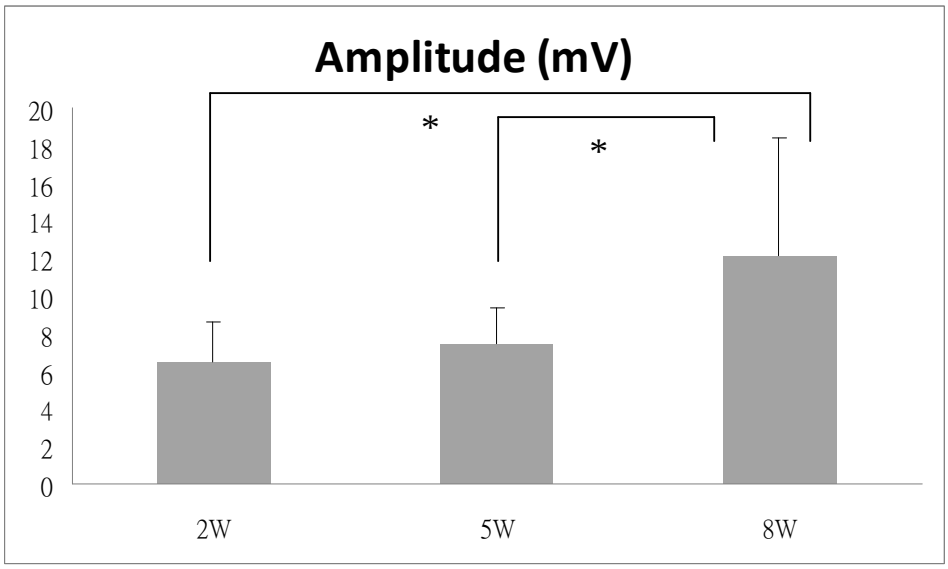
Amplitude (mV)
20
18
16
14
12
10
8
6
4
2
0
*
*
2W
5W
8W

(B)

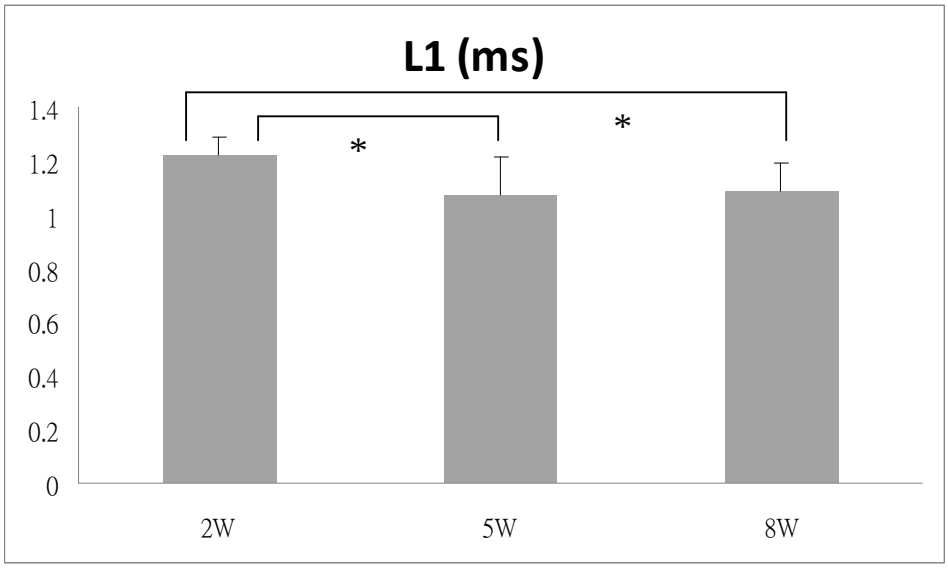
L1 (ms)
1.4
1.2
1
0.8
0.6
0.4
0.2
0
*
*
2W
5W
8W

(C)

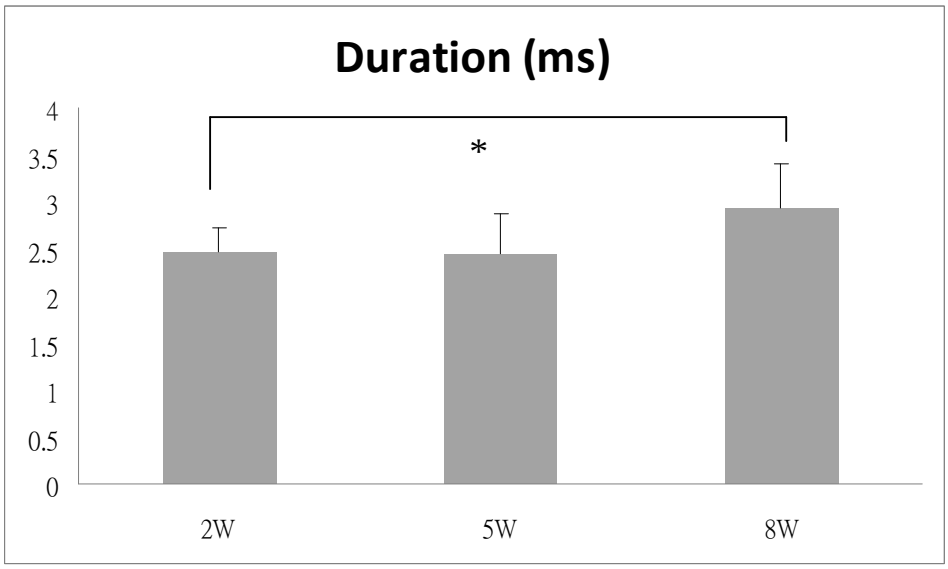
Duration (ms)
4
3.5
3
2.5
2
1.5
1
0.5
0
*
2W
5W
8W

(D)

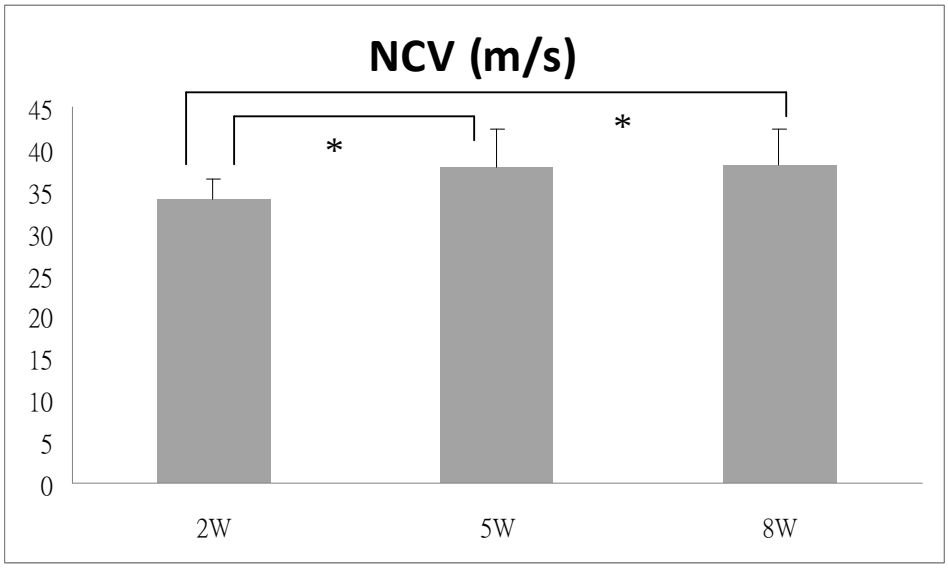
NCV (m/s)
45
40
35
30
25
20
15
10
5
0
*
*
2W
5W
8W

Figure 7

(A)

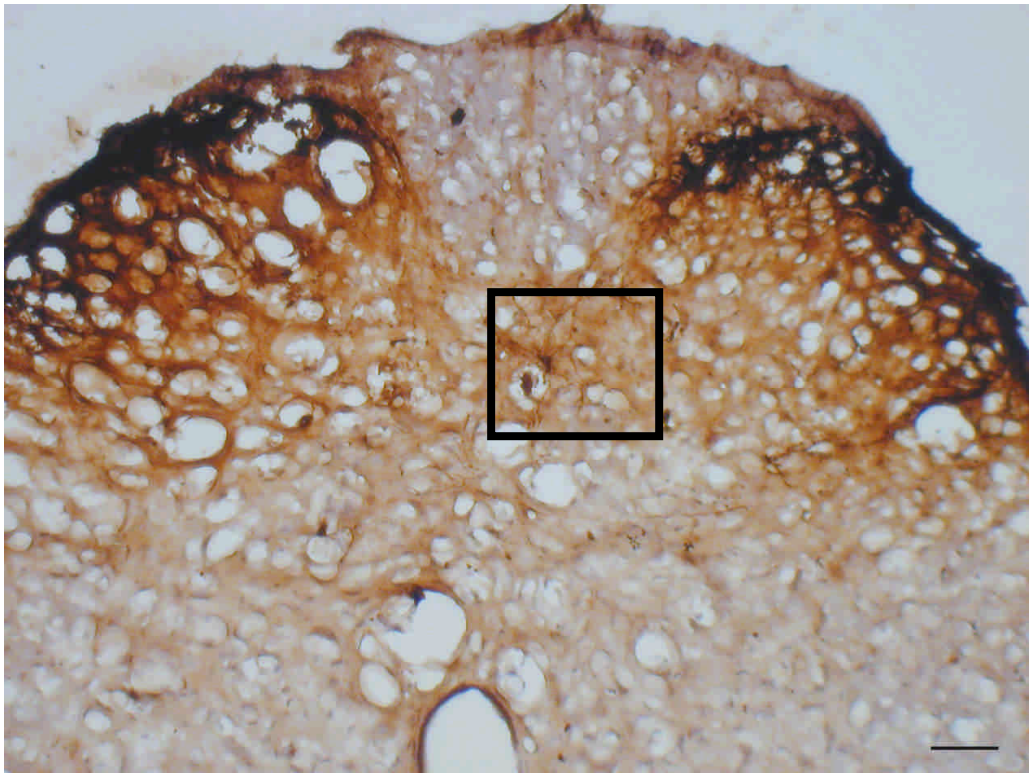

(B)

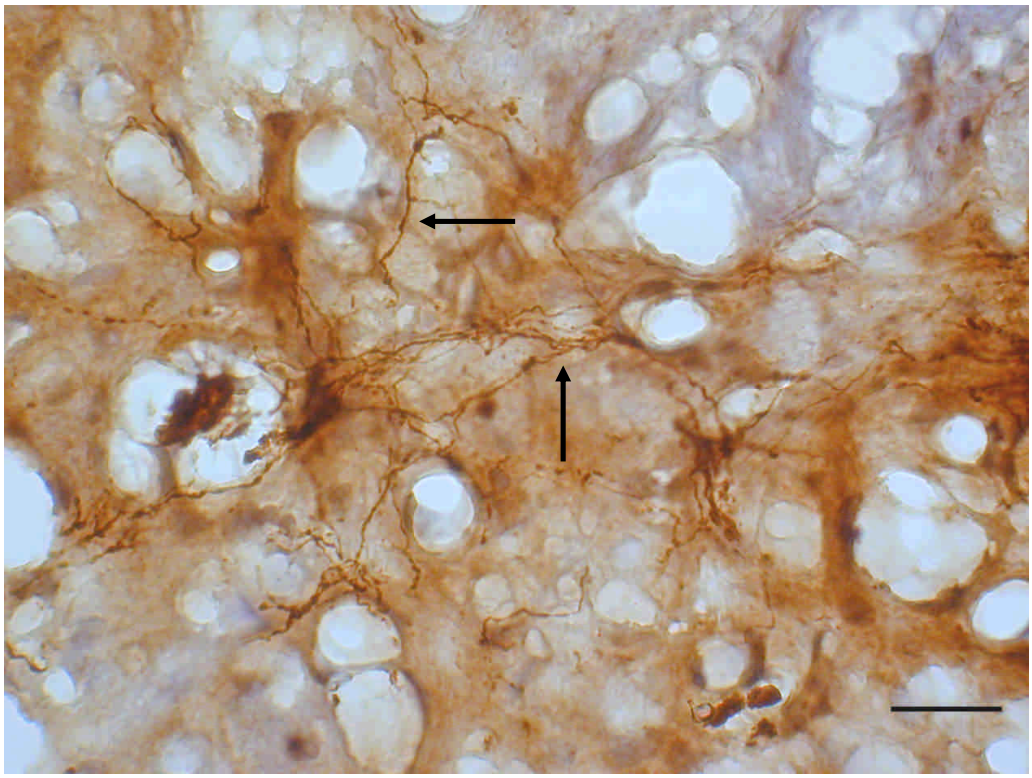

Figure 8

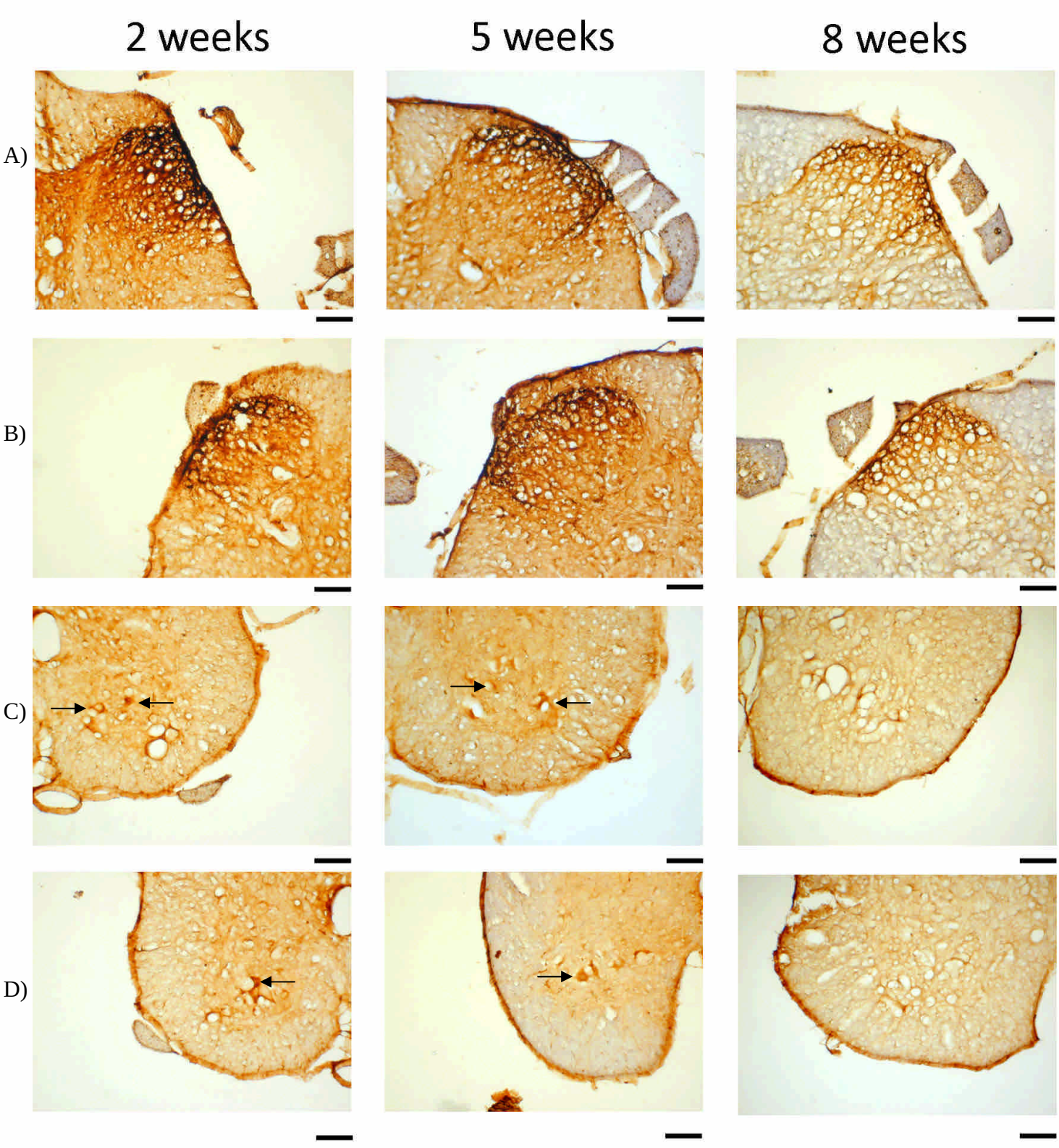

Figure 9

(A)

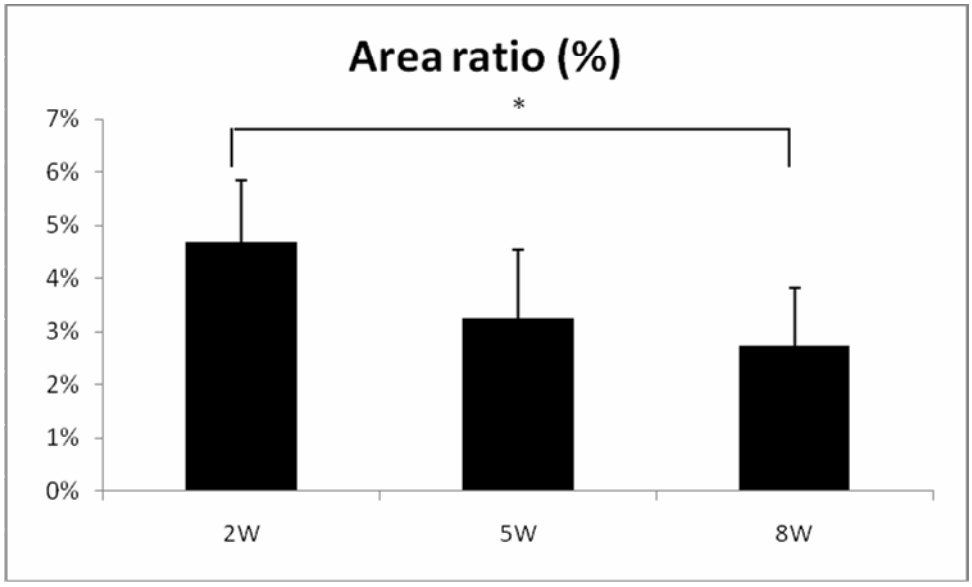

(B)

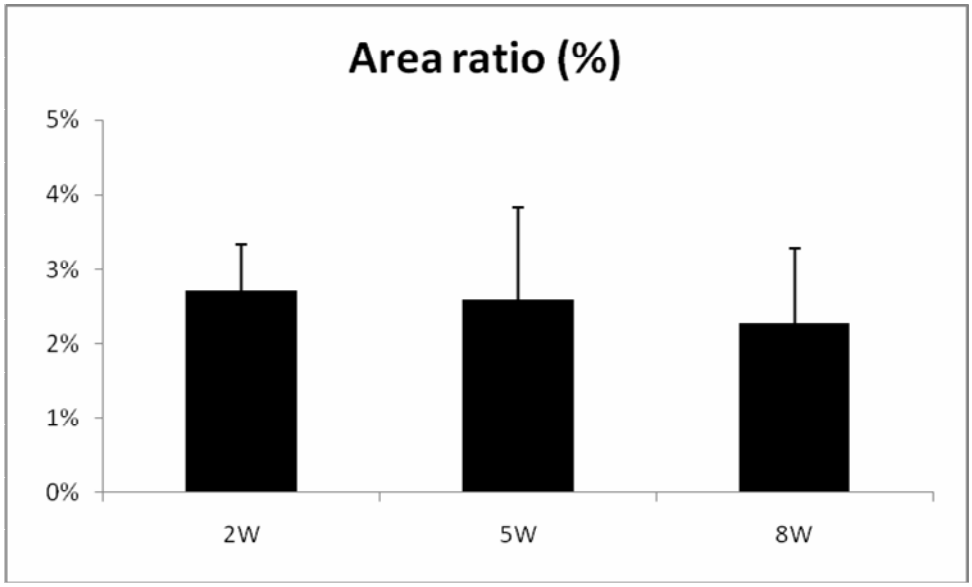

(C)

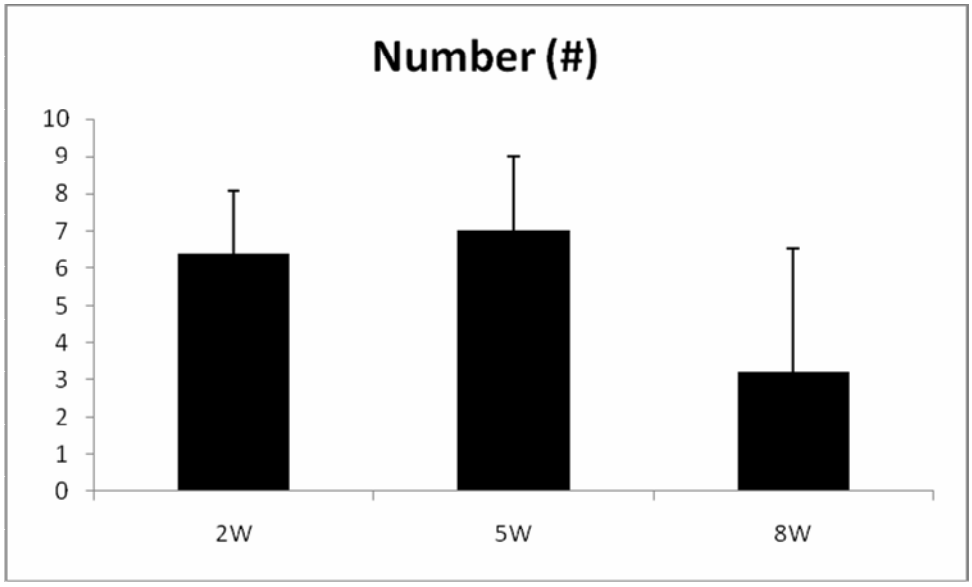

(D)

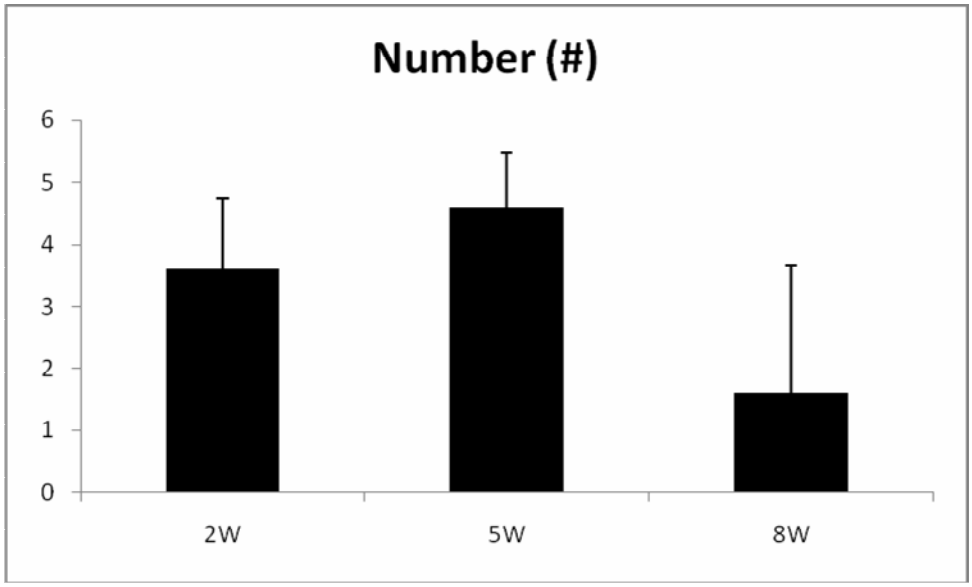

Figure 10

(A)

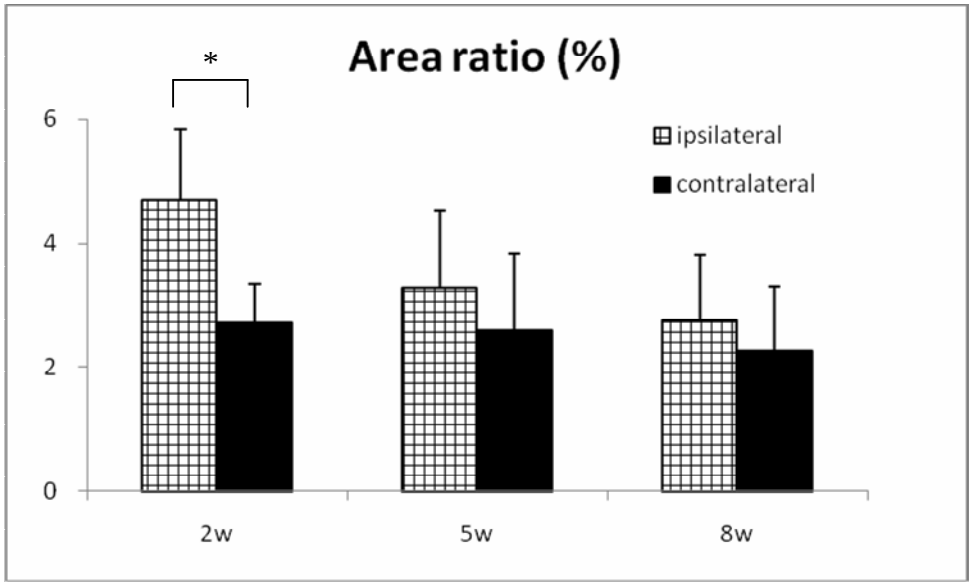
Area ratio (%)
*
6
4
2
0
ipsilateral
contralateral
2w
5w
8w

(B)

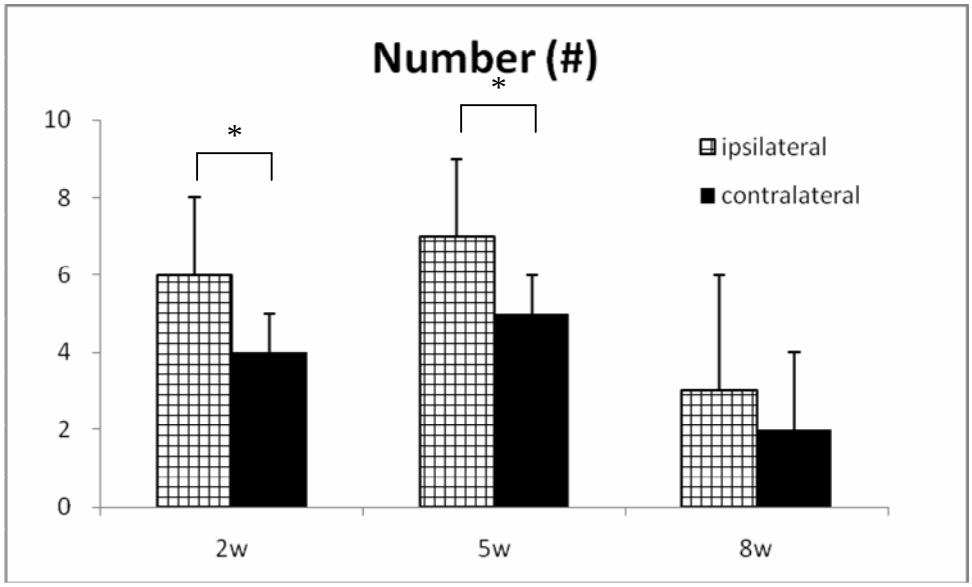
Number (#)
*
*
10
8
6
4
2
0
ipsilateral
contralateral
2w
5w
8w

Figure 11

(A)

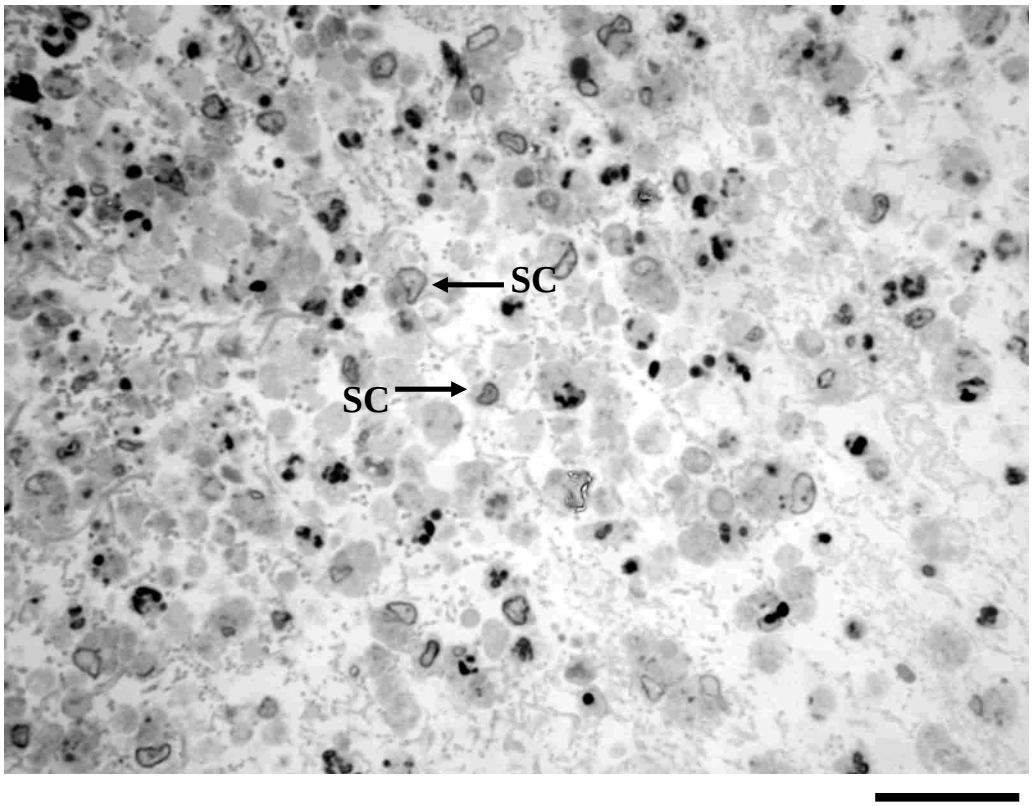

(B)

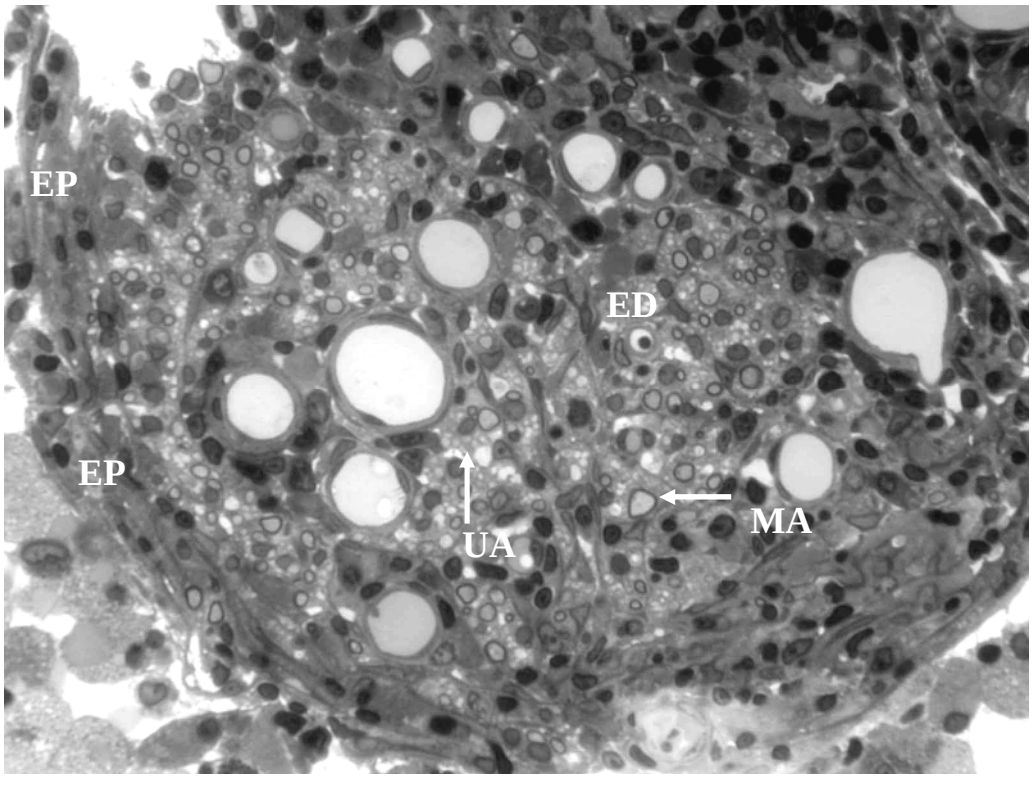

(C)

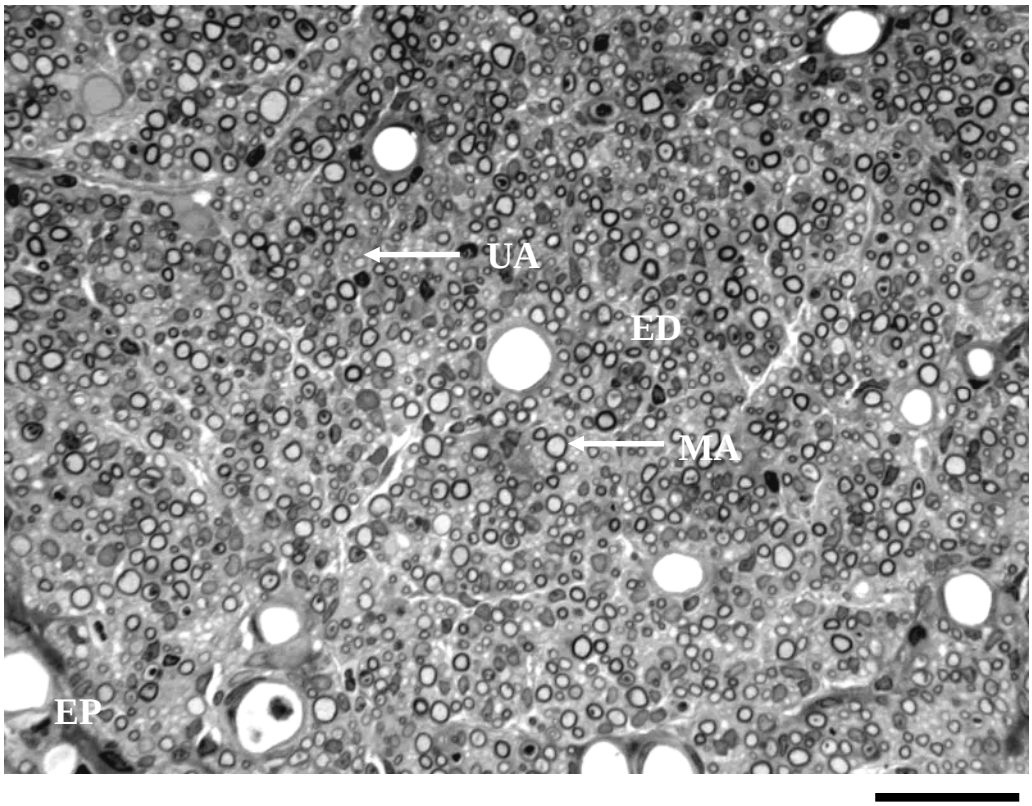

Figure 12

(A)

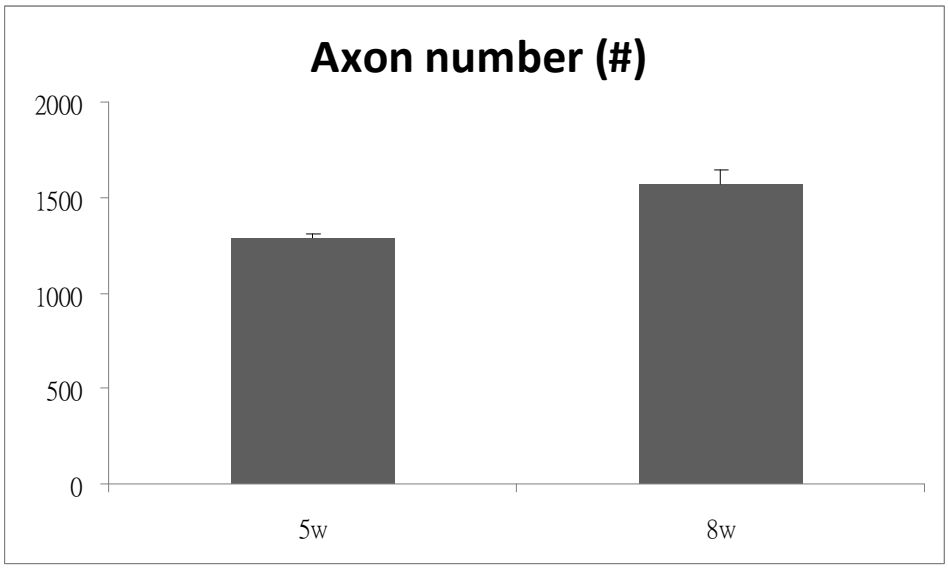
Axon number (#)
2000
1500
1000
500
0
5w
8w

(B)

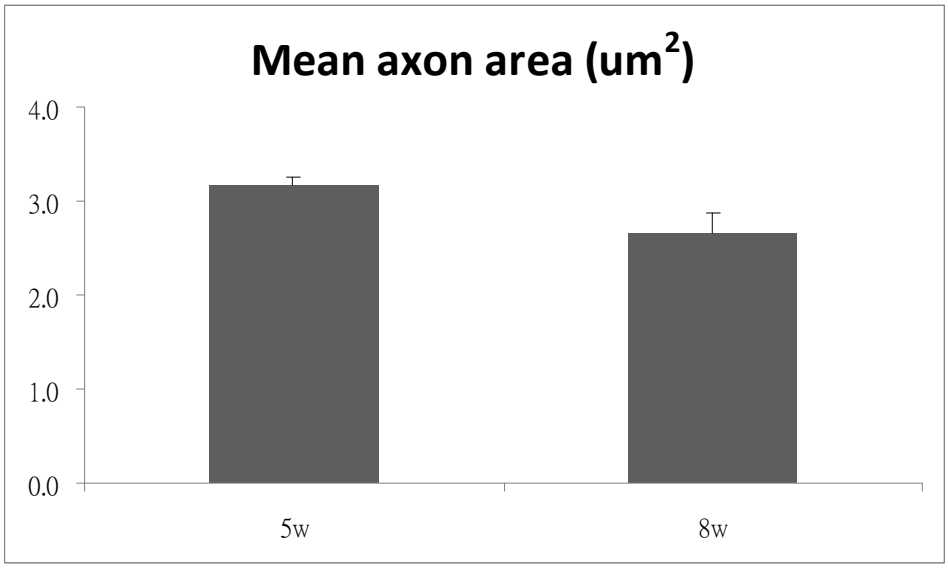
Mean axon area (um2)
4.0
3.0
2.0
1.0
0.0
5w
8w

(C)

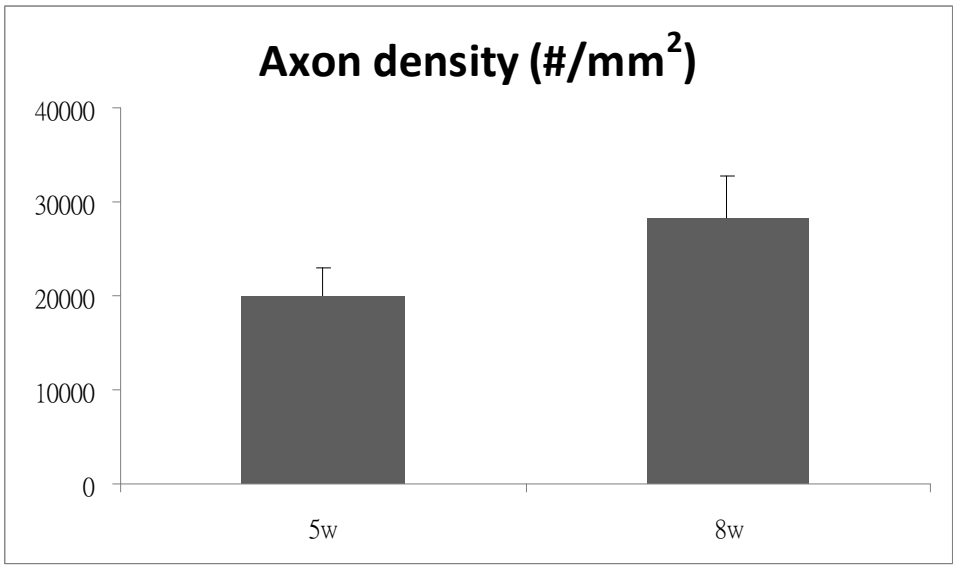
Axon density (#/mm2)
40000
30000
20000
10000
0
5w
8w

(D)

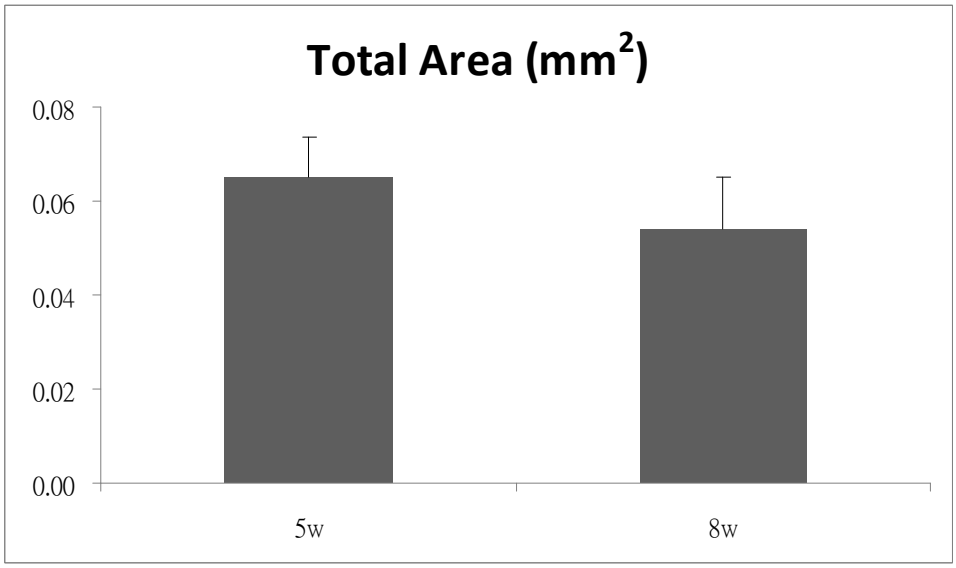
Total Area (mm2)
0.08
0.06
0.04
0.02
0.00
5w
8w

Figure 13

Table of Contents

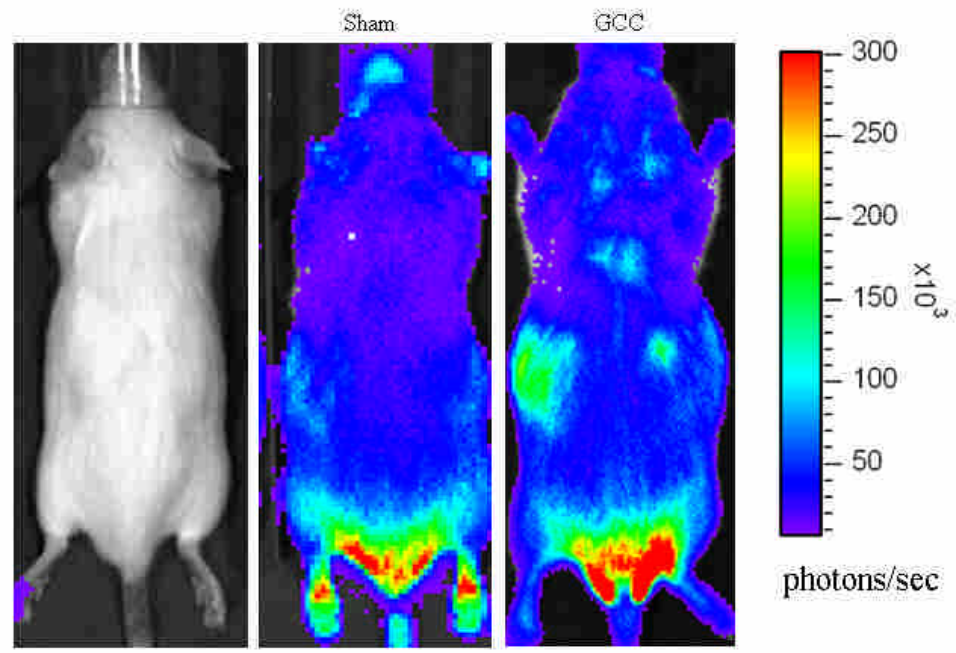

A novel glutaraldehyde-cross-linked casein protein (GCC) conduit was developed. NF-κB-dependent bioluminescence in living mice was used to monitor the immune reponses caused by the implanted GCC conduit. Subsequently, this new protein-based biodegradable conduit was submitted to mechanical, cytotoxic, morphological, and biological tests. Results showed the conduit had properties of great interest towards the repair of regenerating nerve tissues.